deposition was revealed in the enamel of *Col17*$^{-/-}$ incisors from their whitish color and scanning electron microscopy-EDX findings. Iron deposition is known to occur according to the maturation of enamel matrix and mineralization. Thus, reduced iron deposition in the *Col17*$^{-/-}$ mouse incisors suggests defects in enamel maturation and/or mineralization. These results clearly indicate that tooth malformation (amelogenesis imperfecta) in *Col17*$^{-/-}$ mice and probably in *COL17*-deficient nH-JEB patients is caused by aberrant differentiation of ameloblasts. These abnormal ameloblasts lacked Tomes' processes and secreted reduced amounts of enamel matrix irregularly, resulting in disturbed enamel matrix, irregular enamelization and calcification (Figure 7).

We ultrastructurally examined teeth from an adult patient with nH-JEB due to COL17 deficiency using scanning electron microscopy. Enamel rods were malformed and the enamel rod inclination was irregularly oriented and disrupted in the enamel layer of the patient's teeth (data not shown). These abnormalities are most likely a consequence of a lack of COL17 causing aberrant ameloblast differentiation, similar to the *Col17*$^{-/-}$ mice, although we cannot completely exclude the possibility that the morphological changes in the nH-JEB patient's teeth were non-specific abnormalities caused by secondary bacterial infection, etc.

It is reported that heterozygous carriers of glycine substitutions in *COL17A1* show dental abnormalities,[7,20] although such dominant negative mutations in *COL17A1* fail to manifest with a blistering skin phenotype.[20] It is considered that abnormal dentition in the heterozygous carriers is a direct result of dominantly inherited glycine substitutions in *COL17A1* with dominant interference between the wild-type and mutant protein causing ameloblast dysfunction and disruption of enamel deposition.[20] In addition, dental abnormalities were seen both in individuals heterozygous for a *COL17A1* nonsense mutation p.Arg1226X[21] and in heterozygous carriers of a *COL17A1* deletion mutation c.823delA.[7] By contrast, in the present study, *Col17*$^{+/-}$ mice showed no apparent tooth abnormality, probably because the critically disruptive *Col17* allele carried by the mice had no dominant negative effect against wild-type COL17 protein.

Ameloblasts cultured without interaction with mesenchymal tissue cannot differentiate sufficiently to form columnar epithelium.[22] Such insufficiently differentiated ameloblasts express tuftelin, but not other enamel proteins, including amelogenin and ameloblastin.

Ameloblasts in *Col17*$^{-/-}$ mice express tuftelin to an extent similar to that of *Col17*$^{+/+}$ mice, *Col17*$^{-/-}$ ameloblasts express reduced amounts of amelogenin and ameloblastin. Tuftelin is known to be expressed by epithelial cells at a very early stage (the pre-secretory ameloblast stage) of odontogenesis,[23,24] although other major enamel proteins are expressed at the secretory stage.[25] Thus, the results of the present enamel protein expression study further support the idea that ameloblast differentiation from the pre-secretory stage to the secretory stage is disturbed in *Col17*$^{-/-}$ mice.

In the *Col17*$^{-/-}$ mice, ameloblast differentiation was retarded, resulting in malformation of Tomes' processes. The present results in *Col17*$^{-/-}$ mice clearly demonstrated that COL17, a component of the hemidesmosome involved in basement membrane adhesion, also regulates differentiation of odontogenic epithelial cells in ameloblasts and plays and essential role in enamelization.

Laminin 332 is known to be an important component of hemidesmosomes and another causative molecule underlying the JEB phenotype. Remarkable abnormalities, including disturbance of ameloblast differentiation and reduced enamel deposition, have also been reported in the incisors of laminin 332-disrupted mice.[8] These facts further support the idea that interactions between ameloblasts and mesenchymal tissue via hemidesmosomes are crucial for ameloblast differentiation and function.[26,27] Ultrastructural changes of Tomes' processes were not described in laminin 332-disrupted *LAMA3*$^{-/-}$ mice. However, the reduced size of secretory ameloblasts reported in *LAMA3*$^{-/-}$ mice suggest absence or hypoplasia of Tomes' processes in *LAMA3*$^{-/-}$ mice, similar to that observed in *Col17*$^{-/-}$ mice. During the maturation stage, tissue organization was completely disrupted in the enamel epithelium of *LAMA3*$^{-/-}$ mice,[8] but not of *Col17*$^{-/-}$ mice. These findings suggest that a lack of COL17 and a lack of laminin 332 have similar negative effects on ameloblast differentiation and enamel formation, although laminin 332 deficiency appears to have more severe disruptive effects on enamel epithelium, compared with COL17 deficiency.

Our results show that disruption of the *Col17* gene leads to abnormal interaction between enamel epithelium and the underlying mesenchyme via the EMJ, resulting in defective ameloblast differentiation. Consequently, the *Col17*$^{-/-}$ mice exhibit ameloblasts with malformed Tomes' processes and the secretion of enamel matrix was diminished at the secretary stage. At the maturation stage, the *Col17*$^{-/-}$ mice show delayed calcification and reduced iron deposition in the enamel. We consider that these mechanisms contribute to the immature and irregular enamel formation seen in *Col17*$^{-/-}$ mice. In conclusion, epithelial-mesenchymal interactions via the EMJ are important for tooth morphogenesis, and hemidesmosome components are thought to regulate the proliferation and differentiation of tooth forming cells including ameloblasts.

Acknowledgments

We thank Prof. James R. McMillan and Dr. Heather A. Long for their revisions and comments and Dr. Yoshinobu Nodasaka, Mr. Yoshiyuki Honma, and Ms. Kaori Sakai for their fine technical assistance on this project.

References

1. Maas R, Bei M: The genetic control of early tooth development. Crit Rev Oral Biol Med 1997, 8:4–39
2. Liu F, Chu EY, Watt B, Zhang Y, Gallant NM, Andl T, Yang SH, Lu MM, Piccolo S, Schmidt-Ullrich R, Taketo MM, Morrisey EE, Atit R, Dlugosz AA, Millar SE: Wnt/beta-catenin signaling directs multiple stages of tooth morphogenesis. Dev Biol 2008, 313:210–224

3. Borradori L, Sonnenberg A: Structure and function of hemidesmosomes: more than simple adhesion complexes. J Invest Dermatol 1999, 112:411–418
4. McGrath JA, Gatalica B, Christiano AM, Li K, Owaribe K, McMillan JR, Eady RA, Uitto J: Mutations in the 180-kD bullous pemphigoid antigen (BPAG2), a hemidesmosomal transmembrane collagen (COL17A1), in generalized atrophic benign epidermolysis bullosa. Nat Genet 1995, 11:83–86
5. Kirkham J, Robinson C, Strafford SM, Shore RC, Bonass WA, Brookes SJ, Wright JT: The chemical composition of tooth enamel in recessive dystrophic epidermolysis bullosa: significance with respect to dental caries. J Dent Res 1996, 75:1672–1678
6. Nakamura H, Sawamura D, Goto M, Nakamura H, Kida M, Ariga T, Sakiyama Y, Tomizawa K, Mitsui H, Tamaki K, Shimizu H: Analysis of the COL17A1 in non-Herlitz junctional epidermolysis bullosa and amelogenesis imperfecta. Int J Mol Med 2006, 18:333–337
7. Murrell DF, Pasmooij AM, Pas HH, Marr P, Klingberg S, Pfendner E, Uitto J, Sadowski S, Collins F, Widmer R, Jonkman MF: Retrospective diagnosis of fatal BP180-deficient non-Herlitz junctional epidermolysis bullosa suggested by immunofluorescence (IF) antigen-mapping of parental carriers bearing enamel defects. J Invest Dermatol 2007, 127:1772–1775
8. Ryan MC, Lee K, Miyashita Y, Carter WG: Targeted disruption of the LAMA3 gene in mice reveals abnormalities in survival and late stage differentiation of epithelial cells. J Cell Biol 1999, 145:1309–1323
9. Nishie W, Sawamura D, Goto M, Ito K, Shibaki A, McMillan J, Sakai K, Nakamura H, Olasz E, Yancey K, Akiyama M, Shimizu H: Humanization of autoantigen. Nat Med 2007, 13:378–383 in-90
10. Tung K, Fujita H, Yamashita Y, Takagi Y: Effect of turpentine-induced feverduring the enamel formation of rat incisor. Arch Oral Biol 2006, 51:464–470
11. Osawa M, Kenmotsu S, Masuyama T, Taniguchi K, Uchida T, Saito C, Ohshima H: Rat wct mutation induces a hypo-mineralization form of amelogenesis imperfecta and cyst formation in molar teeth. Cell Tissue Res 2007, 330:97–109
12. Fukumoto S, Kiba T, Hall B, Iehara N, Nakamura T, Longenecker G, Krebsbach PH, Nanci A, Kulkarni AB, Yamada Y: Ameloblastin is a cell adhesion molecule required for maintaining the differentiation state of ameloblasts. J Cell Biol 2004, 167:973–983
13. Fukumoto S, Yamada A, Nonaka K, Yamada Y: Essential roles of ameloblastin in maintaining ameloblast differentiation and enamel formation. Cells Tissues Organs 2005, 181:189–195
14. Masuya H, Shimizu K, Sezutsu H, Sakuraba Y, Nagano J, Shimizu A, Fujimoto N, Kawai A, Miura I, Kaneda H, Kobayashi K, Ishijima J, Maeda T, Gondo Y, Noda T, Wakana S, Shiroishi T: Enamelin (Enam) is essential for amelogenesis: eNU-induced mouse mutants as models for different clinical subtypes of human amelogenesis imperfecta (AI). Hum Mol Genet 2005, 14:575–583
15. Jonkman MF, de Jong MC, Heeres K, Pas HH, van der Meer JB, Owaribe K, Martinez de Velasco AM, Niessen CM, Sonnenberg A: 180-kD bullous pemphigoid antigen (BP180) is deficient in generalized atrophic benign epidermolysis bullosa. J Clin Invest 1995, 95:1345–1352
16. Varki R, Sadowski S, Pfendner E, Uitto J: Epidermolysis bullosa. I. Molecular genetics of the junctional and hemidesmosomal variants. J Med Genet 2006, 43:641–652
17. Miletich I, Sharpe PT: Normal and abnormal dental development. Hum Mol Genet 2003, 12:R69–R73
18. Fleischmannova J, Matalova E, Tucker AS, Sharpe PT: Mouse models of tooth abnormalities. Eur J Oral Sci 2008, 116:1–10
19. Smith CE: Cellular and chemical events during enamel maturation. Crit Rev Oral Biol Med 1998, 9:128–161
20. McGrath JA, Gatalica B, Li K, Dunnill MG, McMillan JR, Christiano AM, Eady RA, Uitto J: Compound heterozygosity for a dominant glycine substitution and a recessive internal duplication mutation in the type XVII collagen gene results in junctional epidermolysis bullosa and abnormal dentition. Am J Pathol 1996, 148:1787–1796
21. Floeth M, Bruckner-Tuderman L: Digenic junctional epidermolysis bullosa: mutations in COL17A1 and LAMB3 genes. Am J Hum Genet 1999, 65:1530–1537
22. Morotomi T, Kawano S, Toyono T, Kitamura C, Terashita M, Uchida T, Toyoshima K, Harada H: In vitro differentiation of dental epithelial progenitor cells through epithelial-mesenchymal interactions. Arch Oral Biol 2005, 50:695–705
23. Deutsch D, Leiser Y, Shay B, Fermon E, Taylor A, Rosenfeld E, Dafni L, Charuvi K, Cohen Y, Haze A, Fuks A, Mao Z: The human tuftelin gene and the expression of tuftelin in mineralizing and nonmineralizing tissues. Connect Tissue Res 2002, 43:425–434
24. Leiser Y, Blumenfeld A, Haze A, Dafni L, Taylor AL, Rosenfeld E, Fermon E, Gruenbaum-Cohen Y, Shay B, Deutsch D: Localization, quantification, and characterization of tuftelin in soft tissues. Anat Rec 2007, 290:449–454
25. Fukumoto S, Yamada Y: Extracellular matrix regulates tooth morphogenesis. Connect Tissue Res 2005, 46:220–226
26. Yoshiba K, Yoshiba N, Aberdam D, Meneguzzi G, Perrin-Schmitt F, Stoetzel C, Ruch JV and Lesot H: Expression and localization of laminin-5 subunits during mouse tooth development. Dev Dyn 1998, 211:164–176
27. Fukumoto S, Miner JH, Ida H, Fukumoto E, Yuasa K, Miyazaki H, Hoffman MP, Yamada Y: Laminin alpha5 is required for dental epithelium growth and polarity and the development of tooth bud and shape. J Biol Chem 2006, 24;281:5008–5016

Author's personal copy

chemical-induced carcinogenesis model was chosen in the present study. DMBA and TPA enabled us to produce papillomas within 1–2 months. Furthermore, the number of chemical-induced papillomas was much more than that induced by UVB. Immunohistochemical analyses of skin papillomas using anti-PCNA, -p53, -involucrin, and -keratin antibody, revealed no difference between the chemical- and UVB-induced papillomas (data not shown). Thus the DMBA–TPA-induced mouse skin tumor model was useful to examine the effect of PDT.

In conclusion, EC036-PDT using 670 nm diode laser showed potent anti-tumor effects in DMBA and TPA-induced mouse skin tumor model. EC036-PDT might be more useful than ATX-S10(Na)-PDT for the treatment of skin tumors.

References

[1] Kurwa HA, Barlow RJ. The role of photodynamic therapy in dermatology. Clin Exp Dermatol 1999;24:143–8.

[2] Morton CA, Brown SB, Collins S, Ibbotson S, Jenkinson H, Kurwa H, et al. Guideline for topical photodynamic therapy: report of a workshop of the British Photodermatology Group. Br J Dermatol 2002;143:552–67.

[3] Ormrod D, Javis B. Topical aminolevulinic acid HCl photodynamic therapy. Am J Clin Dermatol 2000;1:133–9.

[4] Tajiri H, Yokoyama K, Boku N, Ohtsu A, Fujii T, Yoshida S, et al. Fluorescent diagnosis of experimental gastric cancer using a tumor-localizing photosensitizer. Cancer Lett 1997;111:215–20.

[5] Nakajima S, Sakata I, Hirano T, Takemura T. Therapeutic effect of interstitial photodynamic therapy using ATX-S10(Na) and a diode laser on radio-resistant SCC II tumors of C3H/He mice. Anticancer Drugs 1998;9:539–43.

[6] Takahashi H, Itoh Y, Nakajima S, Sakata I, Iizuka H. A novel ATX-S10(Na) photodynamic therapy for human skin tumors and benign hyperproliferative skin. Photodermatol Photoimmunol Photomed 2004;20:257–65.

[7] Takahashi H, Nakajima S, Sakata I, Ishida-Yamamoto A, Iizuka H. Photodynamic therapy using a novel photosensitizer, ATX-S10(Na): comparative effect with 5-aminolevulinic acid on squamous cell carcinoma cell line, SCC15, ultraviolet B-induced skin tumors, and phorbol ester-induced hyperproliferative skin. Arch Dermatol Res 2005;296:496–502.

[8] Wolf P, Rieger E, Kerl H. Topical photodynamic therapy with endogenous porphyrin after application of 5-aminolevulinic acid: an alternative treatment modality for solar keratosis, superficial squamous cell carcinoma, and basal cell carcinoma? J Am Acad Dermatol 1993;28:17–21.

[9] Fijian S, Honigsmann H, Ortel B. Photodynamic therapy of epithelial skin tumors using delta-aminolevulinic acid and desferrioxamine. Br J Dermatol 1995;133:282–8.

[10] Calzavara-Pinton PG. Repetitive photodynamic therapy with topical D-aminolevulinic acid as an appropriate approach to the routine treatment of superficial non-melanoma skin tumors. J Photochem Photobiol B 1995;29:53–7.

Hidetoshi Takahashi[a,*], Susumu Nakajima[b], Ryuji Asano[c], Yoshinori Nakae[c], Isao Sakata[c], Hajime Iizuka[a]

[a]*Department of Dermatology, Asahikawa Medical College, 2-1-1-1 Midorigaokahigashi, Asahikawa 078-8510, Japan*
[b]*Moriyama Memorial Hospital, Japan*
[c]*Photochemical Co. Ltd., 5319-1 Haga, Okayama 701-1221, Japan*

*Corresponding author. Tel.: +81 166682523
E-mail address: ht@asahikawa-med.ac.jp
(H. Takahashi)

16 December 2008

doi:10.1016/j.jdermsci.2009.03.008

Letter to the Editor

Higher density of label-retaining cells in gingival epithelium

ARTICLE INFO

Keywords:
Keratinocyte; Oral mucosa; Regeneration; Slow cycling cell; Stem cell

Epithelial sheets made of cultured oral mucosal epithelial cells have been used to treat various epithelial defects [1]. These epithelial sheets are derived from oral epithelial stem cells exhibiting high proliferation potential. In the skin, research into the keratinocyte stem cell niche has advanced remarkably. However, the oral mucosal stem cell niche is less well understood. Thus, we investigated the density of label-retaining cells (LRC) in different areas of oral mucosa to elucidate the localization of oral mucosal stem cells.

Several markers for stem cells have been reported [2]. However, no definite immunohistochemical oral mucosal stem cell marker has yet been established. Stem cells are very slow cycling cells and retain 5-bromo-2′-deoxyuridine (BrdU) label in the nucleus over several weeks [3–5]. Thus, stem cells can be detected as label-retaining cells by BrdU pulse-chase experiments.

We performed BrdU pulse-chase experiments in C57BL/6J mice as previously described [5,6]. For BrdU incorporation studies, the mice ($n = 40$) at 4 weeks of age were given sterile phosphate-buffered saline (PBS) containing BrdU (Roche applied science, Mannheim, Germany) at 0.8 mg/ml. The mice were maintained with PBS drinking fluids containing BrdU for 10 days. Subsequently, the mice were transferred to normal drinking water and five mice were sacrificed every 5 days from 20 days after withdrawal of BrdU-labeling to examine the disappearance of BrdU-labeled cells. Frozen sections were made from the oral mucosal tissue of each mouse and BrdU-positive cells were detected by immunofluorescent stain using anti-BrdU antibody (BrdU Labeling and Detection Kit 1, Roche applied science, Mannheim, Germany).

We studied the slow cycling cells using a label retaining technique in six oral areas; dorsum linguae, inferior surface of the tongue, buccal mucosa, palate, gingiva and alveolar mucosa (Fig. 1). In the areas, the rates of LRC expressed as a percentage of the basal layer oral keratinocytes were examined. On day 1, the next day after the last day of BrdU treatment, the rates of LRCs compared to all basal cells were almost 100% in all areas. The rates of all the areas decreased rapidly and became 10% or less by day 20. In previous studies by Bickenbach and Chism [4] and by Ando et al. [5], LRCs were investigated on day 30 and on day 45, respectively. In addition, after 35 days chasse period, the rate of LRCs of each site seems to reach a plateau (Fig. 2). Thus, we considered that only BrdU-positive cells present after day 35 were LRCs in the present experiments. We performed statistical analysis of LRC rates at day 35 and at day 45.

The rates of BrdU-labeled cells in keratinized regions like the gingiva and the palate were higher than that of other non-keratinized areas from day 20 to day 30 (Fig. 2). These results might reflect a difference in the turnover rates because non-keratinized epithelium has a greater turnover rate than keratinized epithelium [7].

Our study showed that, in thick epithelia forming epithelial ridges, LRCs were seen at the bottom of epithelial ridges (Fig. 1). In contrast, in thin epithelia without epithelial ridges, LRCs were located randomly throughout the basal layer cells.

Author's personal copy

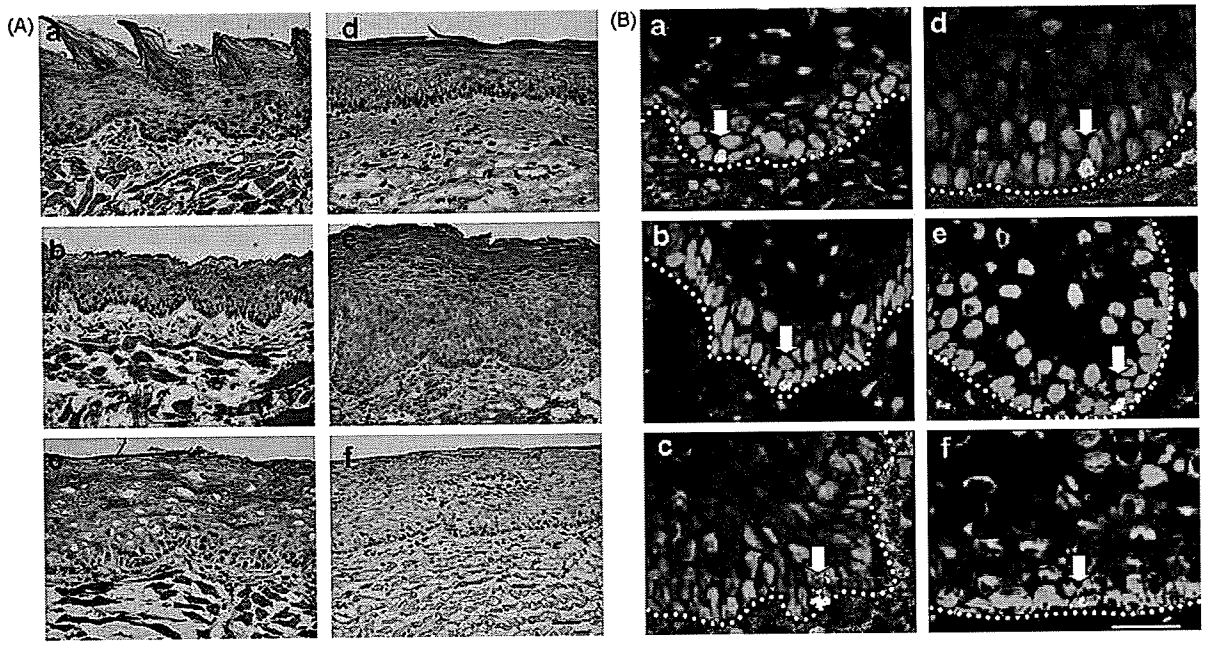

Fig. 1. Localization of label-retaining cells (LRC) in specific regions of oral mucosa. (A) Morphology of each part of oral mucosa (hematoxylin and eosin stain). The epithelium with epithelial ridges was seen in dorsum linguae (a), inferior surface of tongue (b), buccal mucosa (c), and gingiva (e), although the epithelium in palate (d) and alveolar mucosa (f) showed only small epithelial ridges. (B) Immunofluorescent localization of LRCs (arrows) in each part of the oral mucosa at day 50. LRCs were restricted to the basal layer in all the regions. In epithelia with epithelial ridges (panel B-a–c, e), LRCs were seen at the bottom of epithelial ridges. (a) Dorsum linguae, (b) inferior surface of tongue, (c) buccal mucosa, (d) palate, (e) gingival, (f) alveolar mucosa. BrdU labeling, fluorescein isothiocyanate (green); nuclear stain, propidium idodide (red). White dotted line, the basement membrane zone. Bars, 50 μm.

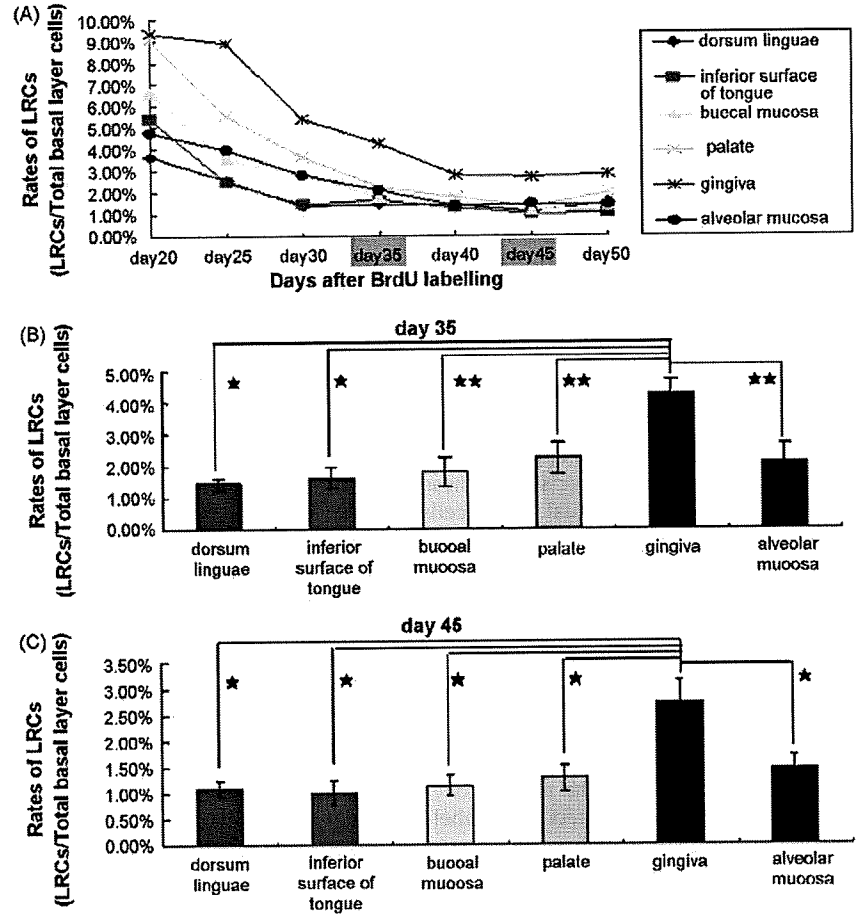

Fig. 2. LRC counts in the oral mucosal epithelium. (A) The rates of BrdU-positive cells to total basal layer keratinocyte numbers from day 20 to day 50. BrdU-positive cells at day 35 and later were considered to be LRCs, the rates of LRCs in the gingiva were significantly higher than those of the other parts in the oral mucosa. (B) Rates of LRCs in each part of oral mucosa at day 35. The rate of LRCs in the gingiva were significantly higher than that in the other parts of the oral mucosa (*$P < 0.05$; **$P < 0.01$). (C) Rates of LRCs in each part of oral mucosa at day 45. As well as day 35, the rate of LRCs in the gingiva were significantly higher (*$P < 0.05$).

Author's personal copy

Interestingly, after day 35, the rates of LRCs in the gingiva were remarkably higher than in the other oral mucosa areas (Fig. 2). At day 35, the rates of LRCs to basal cells were as follows; dorsum linguae, 1.45%; inferior surface of tongue, 1.63%; buccal mucosa, 1.80%; palate, 2.23%; gingival, 4.28%; alveolar mucosa, 2.09%. The existence of LRCs provides no direct indication that such cells are functioning as a subpopulation of stem cells [3]. However, it was thought that the high rates of LRCs in the gingival might reflect a high density of slow-cycling cells, suggesting that there might be a relatively larger number of stem cells in gingival epithelium.

The oral mucosa epithelium comprises stratified squamous epithelium, which may be keratinized or non-keratinized, depending on the region of the oral cavity [1]. The palatal and gingival mucosae are categorized as a masticatory mucosa and their epithelial layer is thick and keratinized or para-keratinized to withstand biting and masticatory stress. The inferior surface of the tongue, buccal mucosa and alveolar mucosa are categorized as a lining mucosa. Their epithelial layers are mostly non-keratinized. The dorsum linguae are classified as a specialized mucosa with several kinds of lingual papillas and their epithelial layers including the filiform papillae show keratinization. The structure of each oral mucosal region in mice was similar to that of the corresponding part in humans.

Examination of hamster palatal papillae showed that the majority of label-retaining cells were located in the deepest part of the epithelial ridges [8]. In this report, any part of oral mucosa epithelium with prominent epithelial ridges had LRCs specifically at the bottom of the ridges without forming a cluster.

The keratinized oral gingival epithelium provides effective protection for underlying tissue against mechanical trauma and dental bacterial invasion. The non-keratinized junctional epithelia with high turnover rates have a basic attachment function to the tooth and form an effective barrier to bacterial penetration [9]. To maintain intact gingiva at the forefront of defense mechanism, a higher density of stem cells might be necessary in the gingival epithelium.

During oral reconstructive surgery, selection of a donor site for mucosal epithelial cell collection is an important agenda. To obtain an epithelial sheet, 15 cm^2 in size, a 4–8 mm^2 mucosal resection is needed [10]. The buccal mucosa has been thought to be an appropriate donor site. Probably collection of the gingival epithelium in surgical procedures such as wisdom tooth extraction and periodontal surgery is a relatively easy way to collect sufficient oral mucosal stem cells. The present results suggest that the gingival epithelium might be a preferable source for collection of oral mucosal epithelial cells for oral mucosal reconstruction treatment.

Acknowledgments

We thank Dr. James R. McMillan for proofreading. This work was supported in part by Grants-in-Aid from the Ministry of Education, Science, Sports, and Culture of Japan to M. Akiyama (Kiban B 20390304).

References

[1] Moharamzadeh K, Brook IM, Van Noort R, Scutt AM, Thornhill MH. Tissue-engineered oral mucosa: a review of the scientific literature. J Dent Res 2007;86:115–24.
[2] Grisanzio C, Signoretti S. p63 in prostate biology and pathology. J Cell Biochem 2008;103:1354–68.
[3] Bickenbach JR. Identification and behavior of label-retaining cells in oral mucosa and skin. J Dent Res 1981;60:1611–20.
[4] Bickenbach JR, Chism E. Selection and extended growth of murine epidermal stem cells in culture. Exp Cell Res 1998;244:184–95.
[5] Ando S, Abe R, Sasaki M, Murata J, Inokuma D, Shimizu H. Bone marrow-derived cells are not the origin of the cancer stem cells in ultraviolet-induced skin cancer. Am J Pathol 2009;174:595–601.
[6] Tough DF, Sprent J. Turnover of naive- and memory-phenotype T cells. J Exp Med 1994;179:127–35.
[7] Thomson PJ, Potten CS, Appleton DR. Mapping dynamic epithelial cell proliferative activity within the oral cavity of man: a new insight into carcinogenesis? Br J Oral Maxillofac Surg 1999;37:377–83.
[8] Bickenbach JR, Mackenzie IC. Identification and localization of label-retaining cells in hamster epithelia. J Invest Dermatol 1984;82:618–22.
[9] Schroeder HE, Listgarten MA. The gingival tissues: the architecture of periodontal protection. Periodontology 2000 1997;13:91–120.
[10] Sauerbier S, Gutwald R, Wiedmann-Al-Ahmad M, Lauer G, Schmelzeisen R. Clinical application of tissue-engineered transplants. Part I. Mucosa. Clin Oral Implants Res 2006;17:625–32.

Takuya Asaka[a,b],
Masashi Akiyama[a,*],
Yoshimasa Kitagawa[b],
Hiroshi Shimizu[a]

[a]*Department of Dermatology, Hokkaido University Graduate School of Medicine, North 15 West 7, Kita-ku, Sapporo 060-8638, Japan*
[b]*Oral Diagnosis and Oral Medicine, Department of Oral Pathobiological Science, Hokkaido University Graduate School of Dental Medicine, Japan*

*Corresponding author. Tel.: +81 11 716 1161x5962; fax: +81 11 706 7820
E-mail address: akiyama@med.hokudai.ac.jp (M. Akiyama)

13 November 2008

doi:10.1016/j.jdermsci.2009.03.006

Letter to the editor

Inhibition of protein kinase CK2 induces E2F1 nuclear export, formation of p21/E2F1 complexes and suppression of DNA synthesis in normal human epidermal keratinocytes

Protein kinase CK2 (formerly termed "casein kinase II") is an extremely conserved Ser/Thr kinase, which is ubiquitously distributed in eukaryotic cells. CK2 is quite unique enzyme, strongly distinguished from others protein kinases by particularly two properties—high constitutive activity and lack of an acute mechanism/s of regulation. The extreme pleiotropy (with list of over 300 substrates) is another of its characteristic [1]. Despite of the gaps in understanding of precise molecular mechanisms the importance of CK2 in the context of signal transduction, gene expression and respectively in the cell regulation, including the maintenance of cell cycle is incontestable.

To gain information about CK2 role in the signal transduction control of keratinocyte cell cycle, we investigated its involvement in the regulation of a crucial transcriptional factors c-Myc and E2F1 by taking advantage of CK2 very selective cell-permeant inhibitor 4, 5, 6, 7-tetrabromobenzotriazole (TBB) (Calbiochem, Darmstadt, Germany).

E2F1 is one of the eight different (E2F1 through -8) members of E2F family of transcription factors, which is essential for cell cycle progression, since it initiates transcription of the genes required for

Clinical and Experimental Dermatology

Usefulness of real-time tissue elastography for detecting lymph-node metastases in squamous cell carcinoma

S. Aoyagi, K. Izumi, H. Hata, H. Kawasaki and H. Shimizu

Department of Dermatology, Hokkaido University Graduate School of Medicine, Sapporo, Japan

doi:10.1111/j.1365-2230.2009.03468.x

Summary

We report a case of invasive SCC arising from multiple lesions of Bowen's disease with right inguinal lymph-node metastasis. Assessment of superficial lymph-node involvement by real-time tissue elastography before surgery was found to be more useful than other noninvasive conventional methods. Histologically, the metastatic tumour cells were located asymmetrically in a small section of the cortical area of the right node, and this result was comparable with the elastographic findings. Additionally, we found that the presence of an asymmetrical cortical area with high elasticity should be included in the determination of metastatic involvement in small lymph nodes. It has high predictive values in the differentiation of benign and malignant superficial lymph nodes in patients with clinically node-negative skin cancer. More cases are needed to validate this efficiency in differentiating benign from malignant lymph-node status, but if confirmed, it may have an important role in the diagnosis of high-risk cutaneous squamous cell carcinoma.

Assessment of superficial lymph-node involvement in patients with cutaneous malignancies before surgery is often difficult. In the inguinal lymph node particularly, swelling from secondary inflammation is often seen in carcinoma arising from the leg. It would be beneficial if differentiation between reactive and metastatic lymph nodes could be made through noninvasive methods. We report the novel use of real-time tissue elastography for the assessment of lymph-node involvement in a patient with invasive squamous cell carcinoma (SCC), and discuss the potential advantages of this technology over other diagnostic techniques.

Report

An 80-year-old Japanese woman presented with a 15-year history of an asymptomatic keratotic plaque on her right lower leg. The lesion had been gradually enlarging, and new small lesions had been arising on her right dorsal foot, thigh and left leg over several months. There was no history of immunosuppression, arsenic exposure or internal malignancy.

On physical examination, a large, red to dark-brown, keratotic plaque measuring 100 mm in diameter was seen on the right pretibial site of the lower leg, with similar multiple small scaly plaques, up to 20 mm in diameter, on both legs (Fig. 1a). The central area of the plaque in the main lesion was markedly raised, with thickened scales and crusting (Fig. 1b). Although there was regional lymphadenopathy in both groins, the clinical appearance suggested secondary inflammation from the regional area, because the nodes felt soft and flat.

A punch biopsy was taken from the large plaque on the right lower leg. The initial histological examination found an intraepidermal neoplasm of atypical keratinocytes characterized by dyskeratotic and mitotic cells. There was no evidence of dermal invasion by tumour cells, indicating a diagnosis of Bowen's disease. Additionally, no evidence of metastasis was found in a computed tomography scan of the whole body including regional lymph nodes at the time of presentation.

Correspondence: Dr Satoru Aoyagi, Department of Dermatology, Hokkaido University Graduate School of Medicine, N15 W7, Kita-ku, Sapporo 060-8638, Japan
E-mail: saoyagi@med.hokudai.ac.jp

Conflict of interest: none declared.

Accepted for publication 29 January 2009

© 2009 The Author(s)

Figure 1 (a) Large, red to dark-brown keratotic plaque measuring 100 mm in diameter on the right pretibial area, with similar multiple small scaly plaques, up to 20 mm in diameter, on both legs; (b) the central area of the lesion on the right pretibial area was markedly raised by thickened scale and crust.

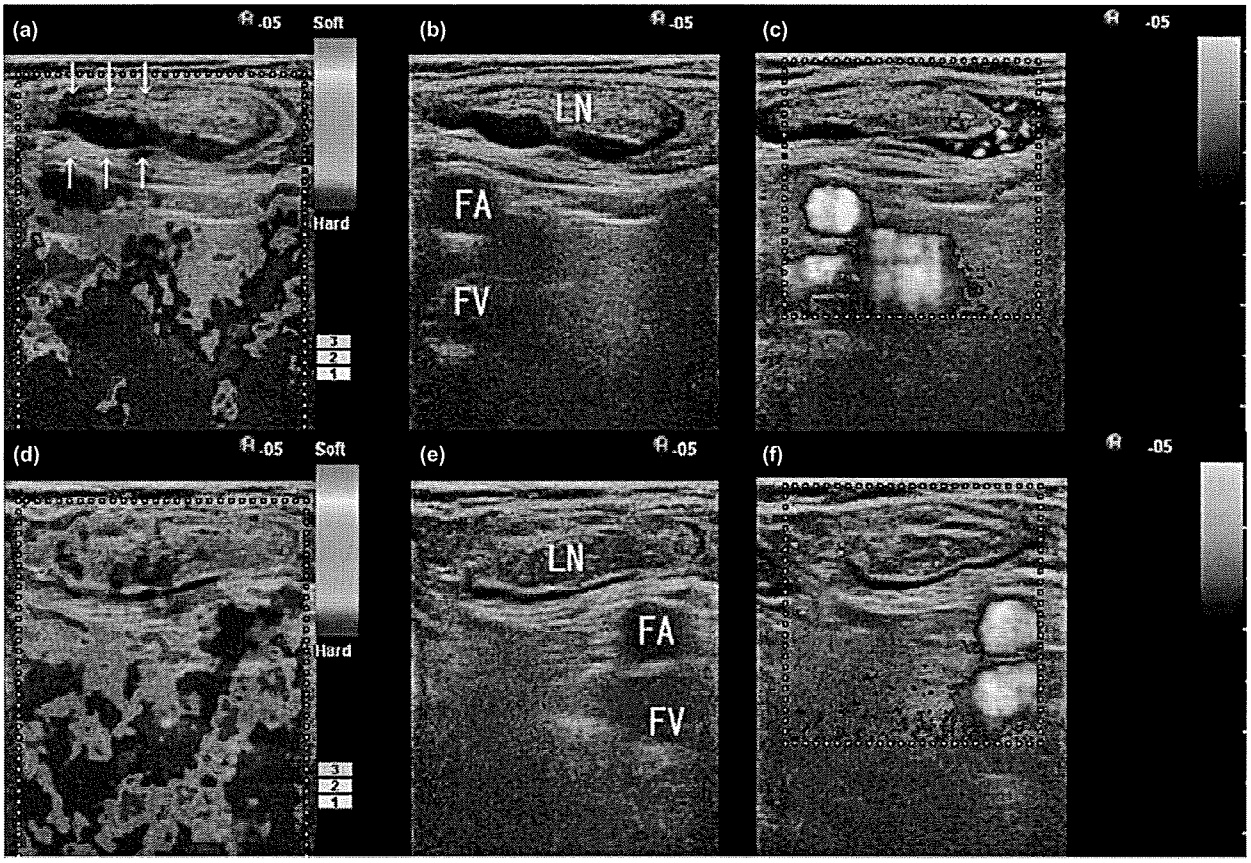

Figure 2 (a–c) Right inguinal lymph node visualized by (a) elastography, showing asymmetrical areas of high elasticity appearing as deep blue in the cortical area (arrows); (b) B-mode sonography; and (c) power Doppler sonography, showing presence of peripheral flow. (d,e) Left inguinal lymph node visualized by (d) elastography, showing several small areas of high elasticity appearing as blue; (e) B-mode sonography; (f) power Doppler sonography, showing weak central hilar and perihilar flow. FA, femoral artery; FV, femoral vein; LN, lymph node.

© 2009 The Author(s)
Journal compilation © 2009 British Association of Dermatologists

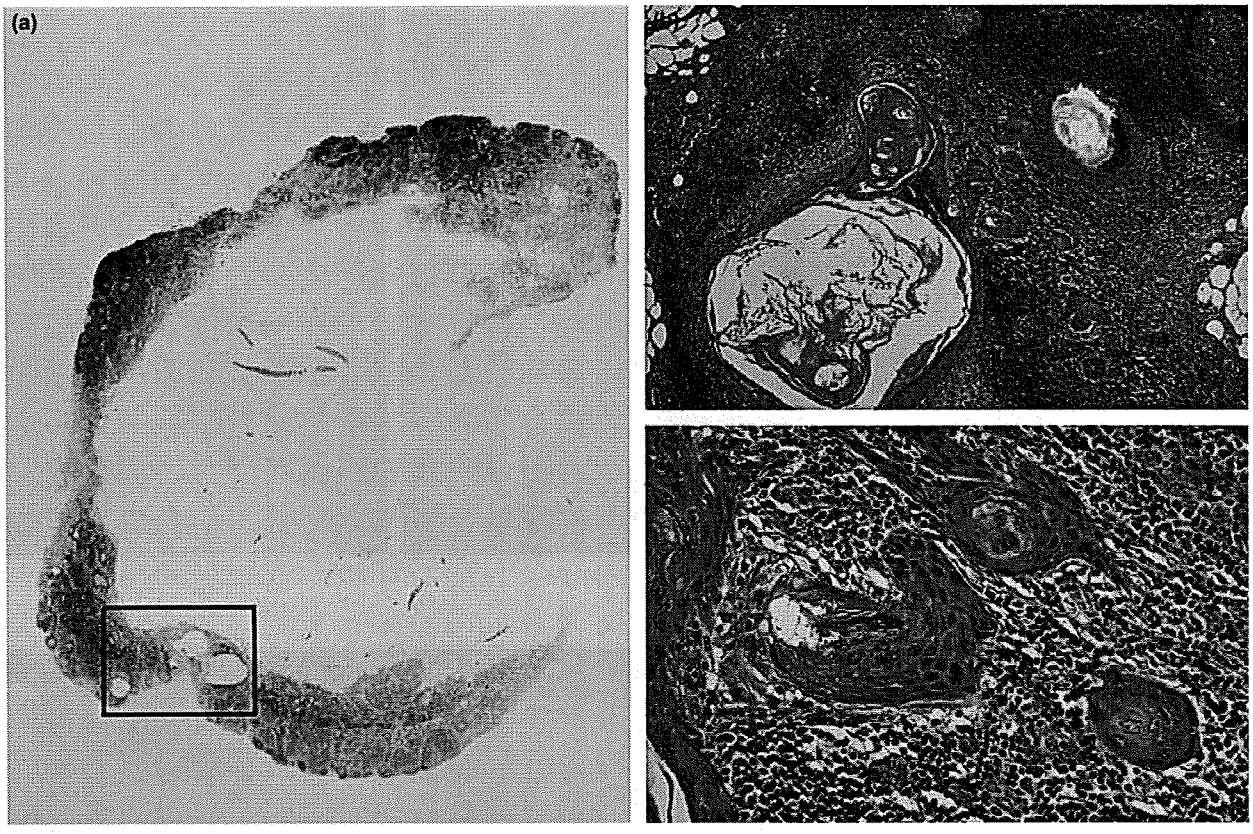

Figure 3 (a) Metastatic area located in a small section of the cortical area, with (b) replacement of the fatty tissue in the centre of the node. (c) Keratinizing squamous differentiation and cell atypia. Haematoxylin and eosin, original magnification (b) × 100 (c) × 200.

The patient underwent ultrasonography (US) examination with a digital sonography scanner (HI VISION 900; Hitachi Medical Corp., Tokyo, Japan) equipped with real-time tissue elastography software (Hitachi Medical). Presence of peripheral flow was seen on Doppler US and an asymmetrical cortical area with high elasticity (appearing as deep blue) on the real-time tissue elastography scan (Fig. 2a–c). These findings were detected only for the right and not the left inguinal lymph node (Fig. 2d–f).

The lesion was excised widely including the underlying fascia and a bilateral inguinal lymph-node biopsy was taken. The surgical specimen showed neoplastic proliferation of differentiated squamous tumour cells with dyskeratotic and atypical keratinocytes throughout the epidermis and into the dermis. The nuclei of the atypical cells were large, pleomorphic and hyperchromatic, with aberrant mitotic nuclei. Invasion of tumour cells into the dermis was seen only in the centre of the lesion. Histological examination of the inguinal lymph-node biopsies confirmed the presence of metastatic tumour cells located asymmetrically in a small section of the cortical area in the right node only (Fig. 3). The left inguinal node was histopathologically confirmed as reactive enlargement.

The final diagnosis of invasive SCC arising from multiple Bowen's disease with right inguinal lymph-node metastasis was made. Because of the right inguinal lymph-node involvement, lymph-node dissection was added to the treatment. The patient was free of disease 4 months after surgery with no recurrence or metastasis.

The development of easy and objective noninvasive methods for the assessment of superficial lymph-node metastasis from cutaneous malignancies would be beneficial in cancer treatment. In evaluating lymph-node metastases, US has several advantages over other conventional imaging methods such as computed tomography, magnetic resonance imaging, scintigraphy and positron emission tomography.[1–3] The characteristic findings for lymph-node metastasis are a low longitudinal and transverse axis ratio (indicating that the shape of the node is round), absence of echogenic

© 2009 The Author(s)

hilum, asymmetrical cortical thickening on usual B-mode US scans, and presence of peripheral flow on Doppler US.[1] However none of these findings is sufficient to replace histopathological examination.

Elasticity is one of the differentiating criteria for metastatic and reactive lymph nodes.[4] In accordance with the hypothesis that solid tumour cells differ in their consistency from adjacent normal tissue,[5] real-time elastography is a new technology for measuring tissue elasticity, using US.[6] It visualizes the differences in tissue strain produced by freehand compression, with tissue appearing on the elastogram as red, yellow, green and blue in ascending order of tissue hardness. Diagnostic use of tissue elastography in breast cancer,[7] thyroid tumour,[8] and lymph-node enlargement in head and neck cancers[9] has already been reported, but to our knowledge, there has been no previous report of diagnostic evaluation of lymph nodes in cases of cutaneous SCC.

According to the previous literature, elastographic patterns are determined by the distribution and percentage of the lymph-node area, with increased tissue hardness appearing as blue areas.[9] The elastographic pattern of our patient shows the blue area corresponding to a reactive node, consistent with this evaluation system (blue area < 45%). The metastatic area was located in a small section of the cortical area and the loss of fatty tissue was seen in the centre of the node, therefore, the lymph node presented as a flattened ring-shaped lesion with an asymmetrical cortical area, with high elasticity appearing as blue and the central low elasticity appearing as red on the elastogram. This finding was not seen in the contralateral inguinal lymph node, which was histopathologically confirmed as a reactive enlargement. Therefore, we suggest that the presence of an asymmetrical cortical area with high elasticity should be included in the elastographic pattern evaluation system for the determination of metastatic involvement in small lymph nodes.

Currently, preoperative determination of metastatic involvement in nonpalpable or small lymph nodes from cutaneous SCC is difficult, and it is still unclear whether surgeons should carry out a lymph-node biopsy or proceed directly to lymph-node dissection. Real-time tissue elastography is a noninvasive and convenient method, especially when combined with Doppler US, which could increase the accuracy of evaluation of metastatic lymph nodes, thus eliminating unnecessary lymph-node biopsy. It also has the potential to detect early metastasis. Further studies are warranted to confirm the usefulness of this technique in tumour evaluation.

References

1 Esen G, Gurses B, Yilmaz MH. Gray scale and power Doppler US in the preoperative evaluation of axillary metastases in breast cancer patients with no palpable lymph nodes. *Eur Radiol* 2005; **15**: 1215–23.

2 Ueda S, Tsuda H, Asakawa H *et al.* Utility of 18F-fluoro-deoxyglucose emission tomography/computed tomography fusion imaging (18F-FDG PET/CT) in combination with ultrasonography for axillary staging in primary breast cancer. *BMC Cancer* 2008; **8**: 165.

3 Sato K, Tamaki K, Tsuda H *et al.* Utility of axillary ultrasound examination to select breast cancer patients suited for optimal sentinel node biopsy. *Am J Surg* 2004; **187**: 679–83.

4 Ueno E, Tohno E, Soeda S *et al.* Dynamic tests in real-time breast echography. *Ultrasound Med Biol* 1988; **14** (Suppl. 1): 53–7.

5 Krouskop TA, Wheeler TM, Kallel F *et al.* Elastic moduli of breast and prostate tissues under compression. *Ultrason Imaging* 1998; **20**: 260–74.

6 Ophir J, Céspedes I, Ponnekanti H *et al.* Elastography. A quantitative method for imaging the elasticity of biological tissues. *Ultrason Imaging* 1991; **13**: 111–34.

7 Thomas A, Fischer T, Frey H *et al.* Real-time elastography – an advanced method of ultrasound: first results in 108 patients with breast lesions. *Ultrasound Obstet Gynecol* 2006; **28**: 335–40.

8 Asteria C, Giovanardi A, Pizzocaro A *et al.* US-elastography in the differential diagnosis of benign and malignant thyroid nodules. *Thyroid* 2008; **18**: 523–31.

9 Alam F, Naito K, Horiguchi J *et al.* Accuracy of sonographic elastography in the differential diagnosis of enlarged cervical lymph nodes: comparison with conventional B-mode sonography. *AJR Am J Roentgenol* 2008; **191**: 604–10.

© 2009 The Author(s)
Journal compilation © 2009 British Association of Dermatologists

J Cutan Pathol 2009: 36: 919–921
John Wiley & Sons. Printed in Singapore

Copyright © 2009 John Wiley & Sons A/S

Journal of
Cutaneous Pathology

Letter to the Editor

Squamous cell carcinoma of the auricle with rhabdoid features

To the Editor,

Squamous cell carcinoma (SCC) is one of the most common malignancies of the external ear. It frequently occurs in elderly people and is associated with a higher metastasis rate, compared to carcinoma found in other locations.[1] As prognoses differ significantly among cutaneous SCC variants,[2] histopathological patterns of individual cases must be carefully examined.

Cutaneous SCC can be classified into several histologic subtypes, differing in prognostic significance.[2] A low-risk subtype includes verrucous SCC and those arising in actinic keratosis. An intermediate-risk subtype consists of adenoid SCC and lymphoepithelioma-like carcinoma. Finally, SCC arising from scars, Bowen's disease with invasion and adenosquamous carcinoma constitute a high-risk subtype. Other rare subtypes, of which a prognosis is not well established, include signet ring cell SCC, follicular SCC, papillary SCC, pigmented SCC, and clear cell SCC. Further studies are required to define the biological behavior and establish a prognostic indication of these rare subtypes of SCC.

Cutaneous SCC with a rhabdoid phenotype is histologically characterized by large cytoplasmic eosinophilic hyaline inclusions with peripheral displacement of vesicular nuclei. Immunohistochemically, these tumor cells show diffused reactivity for cytokeratin and vimentin, which are localized to the cytoplasmic inclusions, but usually not for desmin, smooth muscle actin, or other skeletal muscle markers. To the best of our knowledge, only a few cases of cutaneous SCC with such rhabdoid features have been reported in the literature.[3–6]

An 88-year-old Japanese man presented with an ulcerated reddish colored tumor on the right ear. The tumor, which initially appeared as a small, crusted nodule 2 years ago, had slowly enlarged in size. Bleeding had been occurring from the surface of the tumor for the past 6 months. The past medical history indicates that the patient had been diagnosed with a cerebral infarction and dementia for 3 years. The patient has been taking an anticoagulant agent without any immunosuppressive drug. Physical examination revealed an erosive, fresh-reddish colored, 37 × 25 × 14–mm sized nodule on the right post-auricular shaded area (Fig. 1A). No evidence of regional lymphadenopathy was reported at the time of presentation.

The histological examination of an incision biopsy initially led to the diagnosis of pyogenic granuloma with fibrosis. However, as the small biopsy specimen was taken from a relatively shallow region, the possibility that the nodule represented a case of undifferentiated SCC, could not be completely excluded. Therefore, the lesion was excised widely including cartilage to test for possible malignancy.

The surgical specimen showed dense, dermal and subcutaneous neoplastic proliferation (Fig. 1B) of poorly differentiated tumor cells with numerous plasma cells and histiocytes. The tumor cells consisted predominantly of monomorphic polygonal neoplastic cells, arranged in focally solid sheets (Fig. 2A), particularly in the center of the nodule. The cells possessed abundant eosinophilic, cytoplasmic inclusions with peripheral displacement of the nuclei, characterestic of the rhabdoid phenotype (Fig. 2B). Vascular invasion and lymphatic permeation were not observed. Actinic keratosis in the overlying epidermis was identified only at the border of the nodule as the epidermis was extensively ulcerated.

The tumor cells were tested positive for vimentin and cytokeratin AE1/AE3, but negative for S-100, desmin or smooth muscle actin (SMA). Interestingly, the area tested positive for cytokeratin AE1/AE3 was localized only to the center portion of the lesion (Fig. 2C).

One year after his surgery, the patient remains alive and has not developed any metastatic or recurrent lesions.

Since malignant rhabdoid tumor of the kidney was first described,[7] additional, extra-renal cases have been reported. These cases were regarded as a variant of rhabdomyosarcomatous tumor, based on

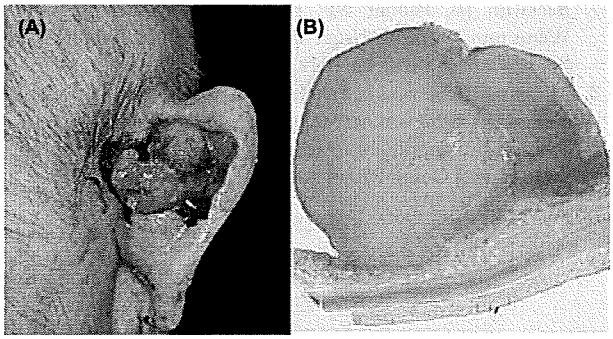

Fig. 1. (A) Clinical features of the tumor. An erosive, fresh-reddish colored, dome shaped nodule on the right post-auricular. (B) Scanning magnification demonstrates that the lesion was well demarcated and showed no evidence of invasion into the underlying cartilage (H&E).

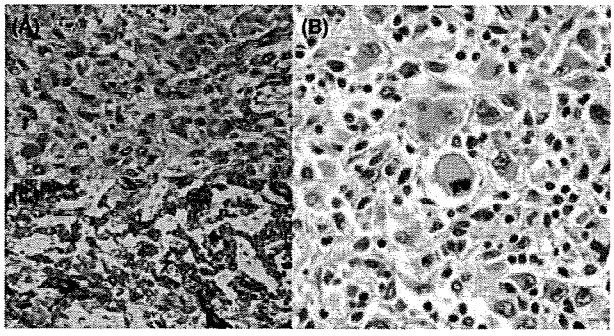

Fig. 2. (A) There were only small areas where the tumor cells formed solid sheets, especially in the center area of the nodule (H&E ×200). (B) Large portions of the tumor cells contained large, globular and cytoplasmic eosinophilic hyaline inclusions that displaced the nuclei peripherally (H&E ×400). (C) Tumor cells located in the center portion of the lesion were strongly positive for cytokeratin AE1/AE3 (×200).

their morphological resemblance to rhabdomyoblasts under a light microscope. However, an ultrastructural examination could not verify the evidence of rhabdomyoblastic differentiation. Later, the rhabdoid morphology thought to be a common endpoint in the origins, because it appeared to be associated with aggressive biological behavior, rapid growth and poor prognosis.[8] According to the close association among rhabdoid features, necrotic cells and debris, this phenotype could represent a phase of degeneration, or a preliminary stage of apoptosis or cell necrosis, rather than a specific type of differentiation.[6] This notion is consistent with the absence of immunohistological reactivity toward skeletal muscle markers in these tumor cells.

Rhabdoid SCC was first described in 1996 by Pai et al.[3] Additional cases have been reported since then, establishing this phenotype as a distinct morphologic variant of cutaneous SCC. Moreover, according to the literature, SCC with rhabdoid features shows a higher degree of recurrence and metastasis than other SCC variants.[6]

The histological examination of our initial biopsy specimen taken from a shallow region of the nodule identified few cellular atypia, numerous inflammation cells, and fibrotic and hemorrhagic tissue, but not neoplastic cells. The lesion was also tested negative for cytokeratin AE1/AE3. Only after the whole histological examination of the larger surgical specimen, the tumor cells were localized in the center portion of the lesion. Furthermore, the lesion was found positive for cytokeratin AE1/AE3, hence leading to a diagnosis as SCC. Therefore, shallow biopsies, as in the case of our first specimen, could increase the risk of misdiagnosing the lesions as a benign tumor.

The lesion was well-demarcated with no evidence of invasion into the underlying cartilage. The low degree of the invasiveness we observed is possibly consistent with the favorable prognosis in our case.

In conclusion, this report introduces characteristic histological patterns that can assist the diagnosis of cutaneous SCC with the rhabdoid features. A biopsy of the deep tissue should be considered crucial for reaching a correct diagnosis. Although our case did not show an aggressive biological behavior, but meaningful discussions on the prognosis of this histological SCC variant await additional investigations.

Satoru Aoyagi, MD, PhD
Hiroo Hata, MD
Maria Maroto Iitani, MD
Erina Homma, MD
Daisuke Inokuma, MD, PhD
Hiroshi Shimizu, MD, PhD
Department of Dermatology, Hokkaido University Graduate School of Medicine,
N15 W7, Kita-ku,
Sapporo, Japan
e-mail: saoyagi@med.hokudai.ac.jp

References

1. Byers R, Kesler K, Redmon B, Medina J, Schwarz B. Squamous carcinoma of the external ear. Am J Surg 1983; 146: 447.
2. Petter G, Haustein UF. Histologic subtyping and malignancy assessment of cutaneous squamous cell carcinoma. Dermatol Surg 2000; 26: 521.
3. Pai SA, Vege DS, Borges AM, Soman CS. Rhabdoid phenotype in squamous carcinoma. A report of two cases. Indian J Cancer 1996; 33: 161.
4. Aljerian K, Alsaad KO, Chetty R, Ghazarian D. Squamous cell carcinoma with rhabdoid phenotype and osteoclast-like giant cells in a renal-pancreas transplant recipient. J Clin Pathol 2006; 59: 1309.

5. Mathers ME, O'Donnell M. Squamous cell carcinoma of skin with a rhabdoid phenotype: a case report. J Clin Pathol 2000; 53: 868.
6. Urdiales-Viedma M, Fernandez-Rodriguez A, De Haro-Muñoz T, Pichardo-Pichardo S. Squamous cell carcinoma of the penis with rhabdoid features. Ann Diagn Pathol 2002; 6: 381.
7. Beckwith JB, Palmer NF. Histopathology and prognosis of Wilms tumors: results from the First National Wilms' Tumor Study. Cancer 1978; 41: 1937.
8. Morgan MB, Stevens L, Patterson J, Tannenbaum M. Cutaneous epithelioid malignant nerve sheath tumor with rhabdoid features: a histologic, immunohistochemical, and ultrastructural study of three cases. J Cutan Pathol 2000; 27: 529.

The American Journal of Pathology, Vol. 174, No. 2, February 2009
Copyright © American Society for Investigative Pathology
DOI: 10.2353/ajpath.2009.080362

Stem Cells, Tissue Engineering and Hematopoietic Elements

Bone Marrow-Derived Cells Are Not the Origin of the Cancer Stem Cells in Ultraviolet-Induced Skin Cancer

Satomi Ando, Riichiro Abe, Mikako Sasaki, Junko Murata, Daisuke Inokuma, and Hiroshi Shimizu

From the Department of Dermatology, Hokkaido University Graduate School of Medicine, Sapporo, Japan

Several lines of evidence have demonstrated that various cancers are derived from cancer stem cells (CSCs), which are thought to originate from either tissue stem or progenitor cells. However, recent studies have suggested that the origin of CSCs could be bone marrow-derived cells (BMDCs); for example, gastric cancer, which follows persistent gastric inflammation, appears to originate from BMDCs. Although our previous research showed the capability of BMDCs to differentiate into epidermal keratinocytes, it has yet to be determined whether skin CSCs originate from BMDCs. To assess the possibility that BMDCs could be the origin of CSCs in skin squamous cell carcinoma (SCC), we used a mouse model of UVB-induced skin SCC. We detected a low percentage of BMDCs in the lesions of epidermal dysplasia (0.59%), SCC *in situ* (0.15%), and SCC (0.03%). Furthermore, we could not find any evidence of clonal BMDC expansion. In SCC lesions, we also found that most of the BMDCs were tumor-infiltrating hematopoietic cells. In addition, BMDCs in the SCC lesions lacked characteristics of epidermal stem cells, including expression of stem cell markers (CD34, high α6 integrin) and the potential retention of BrdU label. These results indicate that BMDCs are not a major source of malignant keratinocytes in UVB-induced SCC. Therefore, we conclude that BMDCs are not the origin of CSCs in UVB-induced SCC. ***(Am J Pathol 2009, 174:595–601; DOI: 10.2353/ajpath.2009.080362)***

Stem cells, which have the capacity to self-renew and to differentiate into the various mature cells that constitute the tissue of organ, are found in many adult tissues including the skin.[1] Stem cells are critical for replenishing and maintaining the balance of cells (homeostasis) within the tissue and reconstituting tissue damaged during injury. Numerous studies have shown that the specific stem cell properties and the characteristics of stem-cell systems (populations of cells that derive from stem cells are organized in a hierarchical manner) are relevant to some forms of human cancer.[2,3] In cancers, cancer stem cells (CSCs) are thought to exist. CSCs, like tissue stem cells, would have a capacity for self-renewal and a proliferative ability with successive expansion potential promoting tumor structure organization Tumor-initiating cells, which are considered to be a population rich in CSCs, have been identified in cancers of the hematopoietic system[4,5] and various organs.[6–10]

Although several lines of evidence indicate that CSCs can arise from tissue stem cells[6,8,11,12] or mutated progenitor cells[13,14] current reports showed that gastric cancer, which follows persistent gastric inflammation because of the infection with *Helicobacter felis* (*H. felis*), appears to originate from bone marrow-derived cells (BMDCs).[15] Indeed, some populations of BMDCs have the potential to differentiate into mature cells of various nonhematopoietic organs including liver,[16] skeletal-muscle,[17] brain,[18] and skin.[19] We also showed that BMDCs and mesenchymal stem cells are able to transdifferentiate into keratinocytes.[20,21] BMDCs with this plasticity are frequently recruited to sites of injured or inflamed tissue, where they differentiate into mature tissue cells to contribute to tissue repair.[22] Results from *H. felis*-induced gastric cancer suggest that BMDCs with plasticity would differentiate into tissue stem or mature cells to reconstitute the damaged tissue, they then covert into CSCs, and contribute to carcinoma formation. Although recent investigations have demonstrated that BMDCs could contribute to cancers of small intestine, colon, lung,[23] larynx, and brain,[24] it is yet to be determined whether cancers originating from BMDCs certainly exist.

Accepted for publication November 4, 2008.

Address reprint requests to Hiroshi Shimizu, M.D., Ph.D., or Riichiro Abe, M.D., Ph.D., Department of Dermatology, Hokkaido University Graduate School of Medicine., N 15 W 7, Kita-ku, Sapporo 060-8638, Japan. E-mail: shimizu@med.hokudai.ac.jp and aberi@med.hokudai.ac.jp.

Skin cancer is currently the most common malignancy in humans.[25] The skin has the role to protect our bodies from a wide range of environmental assaults including UVB irradiation, chemical carcinogens, and the entry of viruses and other pathogens. Therefore, epidermal keratinocytes have more opportunity to manifest maturation arrest. Particular epidemiological and scientific evidence has shown that UVB is one of the most important factors affecting skin carcinogenesis in the physical environment.[25,26]

As in the case of BMDC-originated gastric cancer after persistent inflammation with *H. felis* infection, it is presumed that BMDCs, which are recruited to the UVB-damaged epidermis and differentiate into epidermal keratinocytes to reconstitute the damaged skin, could then give rise to the maturation arrest during continuous UVB irradiation, convert into CSCs, and finally propagate to form bone marrow (BM)-derived skin cancer. Such a novel hypothesis, if true, would have profound implications for our present understanding of the pathogenesis of squamous cell carcinoma (SCC).

To investigate the possible role of BMDCs in skin cancer, we used a mouse model of UVB-induced skin SCC and evaluated the number and marker expressions of labeled BMDCs that differentiated into keratinocytes in skin SCC.

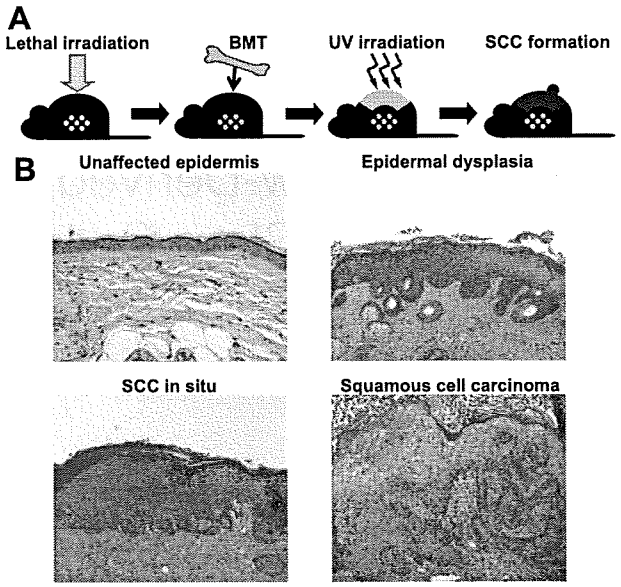

Figure 1. UVB-induced SCC model mice in which BMDCs are labeled with β-Gal enzyme or GFP. **A:** Lethally irradiated mice were transplanted with BM from ROSA26 mice expressing β-Gal enzyme or GFP mice expressing GFP. After confirmation of BM reconstitution, mice were UVB-irradiated. Intermittent UVB irradiation leads mice skin to form SCC. **B:** Tumors were histologically classified as unaffected, dysplasia, SCC *in situ*, or SCC based on tumor architecture, keratinocyte differentiation, and cytological atypia.

Materials and Methods

BM Transplantation

All animal procedures were conducted according to the guidelines of the Hokkaido University Institutional Animal Care and Use Committee under an approved protocol. BM was isolated from the femurs and tibias of male C57BL/6JGtrosa26 (ROSA26) or C57BL/6-TgN(ACTB-EGFP)1Osb/J (GFP) mice (The Jackson Laboratory, Bar Harbor, ME). After lethal irradiation (9 Gy), 1×10^6 BM cells from donor mice in a volume of 200 μl of sterile phosphate-buffered saline were transplanted to recipient C57BL/6 female mice via a single tail vein injection. Hematopoietic reconstitution was subsequently evaluated in peripheral blood 4 weeks after transplantation and more than 94% of BM cells were donor-derived cells.

Induction of UVB Radiation-Induced SCC

UVB-induced carcinogenesis was performed as previously reported (Figure 1A).[27] The UVB light source was a FL20SE30 fluorescent lamp (Clinical Supply, Tokyo, Japan). The UVB irradiation (180 mJ/cm^2) was continued daily for 10 days for tumor initiation to mice (n = 20). One week after the initiation, UVB exposure (180 mJ/cm^2) was performed twice a week until the end of the experiment at 10 months from the last UVB exposure. At 5 months, all irradiated mice (n = 8) had small papules (at least two papules) and erosion. At 10 months, all irradiated mice (n = 6) had tumors (at least three tumors), papules (at least five papules), and ulcer.

Histological Analysis

Mice were sacrificed and tissue was removed, embedded in OCT compound (Sakura, Torrance, CA), snap-frozen or fixed in 4% formalin, and embedded in paraffin. Tumor sections were visualized by routine staining with hematoxylin and eosin (H&E). All of the slides were reviewed twice in blinded manner by three dermatologists, and assessed for tumor architecture, keratinocyte differentiation, cytological atypia, and inflammation. Tumors were classified as dysplasia (typical papilloma), SCC *in situ*, or SCC based on tumor architecture and cytological atypia as described previously.[28] Some lesions exhibiting nonpapillomatous architecture and comprising one to three layers with well-differentiated keratinocytes were classified as normal. Ten samples were analyzed in each normal growth, dysplasia, SCC *in situ*, and SCC. Counts were averaged from eight or nine separate fields in each histological category.

Determination of Enzyme (X-Gal) Activity

Frozen sections (5 μm) were fixed for 30 minutes in 0.2% glutaraldehyde, washed in sodium phosphate buffer containing 0.01% sodium deoxycholate and 0.02% Nonidet P-40 and 1 mmol/L MgCl and incubated for 10 hours at 37°C in a 1-mg/ml X-Gal solution [5-bromo-4-chloro-3-indolyl-β-galactopyranoside: X-Gal, dissolved in dimethyl sulfoxide, 5 mmol/L $K_3Fe(CN)_6$, 5 mmol/L $K_4Fe(CN)_6$ $3H_2O$ in 0.1mol/L sodium phosphate buffer] and counterstained with H&E.

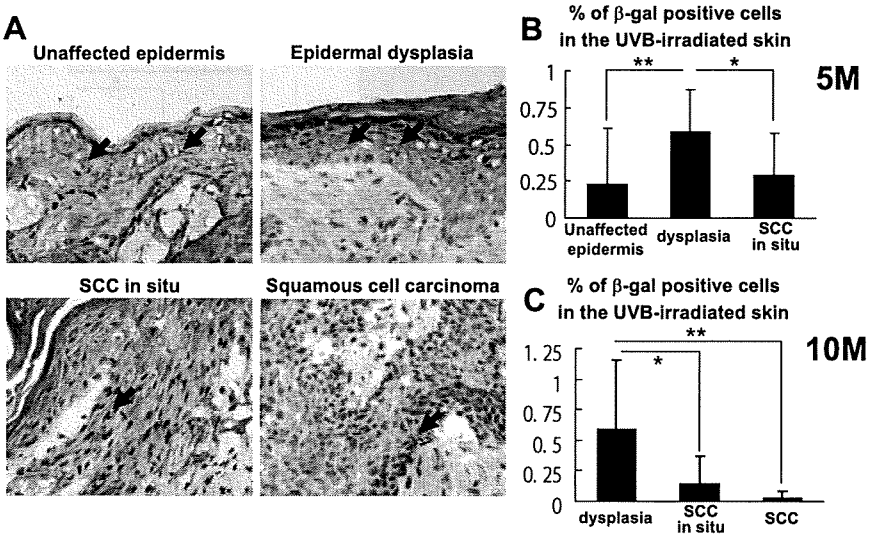

Figure 2. BMDCs in UVB-irradiated mouse skin. **A:** X-Gal-positive cells located within the basal layer in the unaffected epidermis lesions. In the epidermal dysplasia lesions, most X-Gal-positive cells (**arrows**) were found in the suprabasal layers. In the SCC *in situ* lesions, X-Gal-positive cells were found at the inner part of the tumor. In the SCC lesions, X-Gal-positive cells were also found at the inner part of the tumor. **B:** After 5 months of UVB irradiation, the percentage of X-Gal-positive cells was found at 0.15 ± 0.21% in the unaffected epidermis lesions, increased to 0.58 ± 0.25% in the epidermal dysplasia lesions, and decreased to 0.25 ± 0.20% in the SCC *in situ* lesions (*$P < 0.05$, **$P < 0.01$). **C:** After 10 months of UVB irradiation, the percentage of X-Gal-positive cells was 0.59 ± 0.57% in the epidermal dysplasia lesions and 0.15 ± 0.22% in the SCC *in situ* lesions. In the SCC lesions, the percentage of X-Gal-positive cells in the tumor was decreased to 0.03 ± 0.06% (*$P < 0.05$, **$P < 0.01$).

Immunofluorescence

Frozen blocks were prepared and sectioned as described above. Sections were fixed in 4% paraformaldehyde and analyzed for β-galactosidase-expressing cells by using polyclonal antibodies (Cappel, Aurora, OH) and fluorescent secondary antibodies (fluorescein isothiocyanate-labeled goat anti-rabbit antibody; Jackson ImmunoResearch, West Grove, PA). Sections fixed in 4% paraformaldehyde were also analyzed for GFP-expressing cells by using polyclonal antibodies (Molecular Probes, Carlsbad, CA). β-Galactosidase-expressing cells were also stained with antibodies to CD45 (BD Biosciences, San Diego, CA), pan cytokeratins (Progen, Heidelberg, Germany), CD34 (BD Biosciences), or α6 integrin (BD Biosciences). Sections ware viewed with a confocal laser-scanning fluorescence microscope (FV1000; Olympus, Tokyo, Japan).

BrdU Assay

The procedure for BrdU pulse labeling and the subsequent detection were performed as previously reported.[29] In brief, at the time of 9-month UVB irradiation, the tumor-bearing model mice were fed with water containing BrdU (1 mg/ml) for 10 days. Forty-five days after BrdU labeling, the tissues were removed. Frozen sections were fixed with 4% paraformaldehyde or 70% ethanol, stained with antibodies to BrdU (Roche, Penzberg, Germany) and fluorescent second antibodies (tetramethyl-rhodamine isothiocyanate-labeled goat anti-mouse antibody; Southern Biotechnology, Birmingham, AL).

Fluorescence in Situ *Hybridization*

X and Y chromosomes were detected on sections from the UVB-irradiated mice skin using a dual-color detection kit (Cambio, Cambridge, UK) according to the manufacturer's protocol (Cy5 for Y chromosomes and Cy3 for X chromosomes) and immediately viewed with a confocal microscope.

Results

Low Frequency of BMDCs in UVB-Irradiated Skin

To investigate the possible role of BMDCs in UVB-induced skin dysplasia/carcinoma progression, we used a model mouse whose BMDCs are labeled with β-galactosidase (β-Gal) or green fluorescent protein (GFP). Lethally irradiated mice were transplanted with BM from ROSA26 mice or GFP transgenic mice (Figure 1A). After the confirmation of BM reconstitution, mice were irradiated with UVB and developing tumors in mice skin were evaluated histologically. Each section was divided into four categories of unaffected, dysplasia, SCC *in situ*, and SCC (Figure 1B).[28] After 5 months of UVB irradiation, we found the dysplasia lesions and the SCC *in situ* lesions, whereas we found no SCC lesions in irradiated skin. After 10 months of UVB irradiation, the dysplasia lesions and the SCC *in situ* lesions were found to be continuous with the SCC lesions, whereas the unaffected epidermis lesions were completely absent.

To detect the presence of BMDCs in UVB-irradiated mouse skin, X-galactosidase (X-Gal) staining was performed. The numbers of BMDCs were quantified by counting the number of X-Gal-positive cells in the UVB-irradiated mouse skin (Figure 2A). After 5 months of UVB irradiation, even in the unaffected epidermis lesions, some X-Gal-positive cells, indicating BMDCs, were located within the basal layer. In the epidermal dysplasia lesions, some X-Gal-positive cells were also found within the basal layer, but most X-Gal-positive cells were found within the suprabasal layers. In the SCC *in situ* lesions, X-Gal-positive cells were found within the inner parts of the tumor. The percentage of occurrence of X-Gal-positive cells was 0.15% in the unaffected epidermis lesions. Since we previously showed that wounded skin contained BMDCs (0.03%),[20] repeated UVB irradiation might induce BMDC accumulation. The percentage of X-Gal-positive cells in the epidermal dysplasia lesions increased to 0.58%, whereas the percentage of X-Gal-

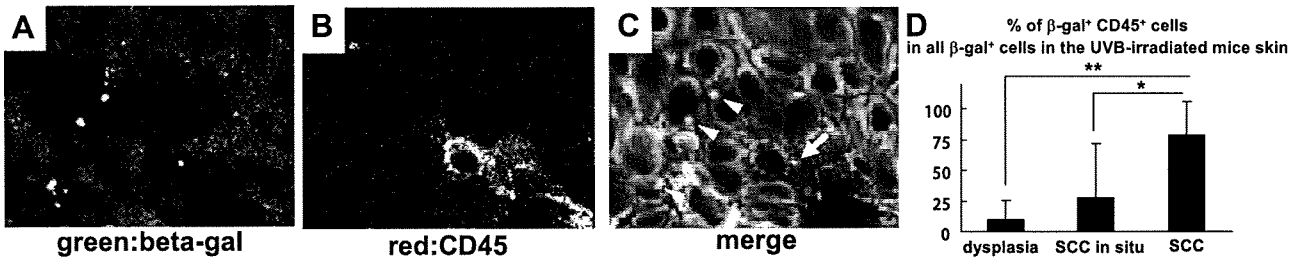

Figure 3. BM-derived infiltrating cells in the UVB-irradiated skin. Triple staining of β-Gal (green) (**A**), CD45 (red) (**B**), and pancytokeratin (cyan) was performed. **C:** Merged image showed β-Gal$^+$/CD45$^+$ (**arrow**) or β-Gal$^+$/CD45$^-$ (**arrowheads**) cells in the tumor. **D:** Percentage of CD45$^+$ of all β-Gal$^+$ cells in the UVB-irradiated mice skin. In all β-Gal$^+$ cells, 10.1 ± 15.3% was positive for CD45 in the epidermal dysplasia lesions, 27.3 ± 44.1% in the SCC *in situ* lesions, and at 78.7 ± 27.4% in the SCC lesions ($^*P < 0.05$, $^{**}P < 0.01$). Original magnifications, ×600.

positive cells in the SCC *in situ* lesions was decreased to 0.25% (Figure 2B). The number of β-Gal-positive cells and total epidermal cells of the UVB-irradiated skin were as follow; unaffected (6 of 2276), dysplasia (28 of 4804), SCC *in situ* (15 of 5445). We further confirmed that no X-Gal-positive cells were detected in untreated (unirradiated) mice. We failed to find any clusters of X-Gal-positive cells in either the unaffected epidermis or the tumor. These results indicate that BMDCs in the UVB-irradiated skin do not commonly give rise to a monoclonal expansion.

After 10 months of UVB irradiation, in the epidermal dysplasia lesions and SCC *in situ* lesions, we found X-Gal-positive cells in a similar location as mice skin that received 5 months of UVB irradiation. In the SCC lesions, X-Gal-positive cells were found within the inner part of the tumor (Figure 2A). X-Gal-positive cells were found at a percentage of 0.59% in the epidermal dysplasia lesions and 0.15% in the SCC *in situ* lesions. These percentages of X-Gal-positive cells in 10-month UVB-irradiated mouse skin were similar to the percentage in 5-month UVB-irradiated mouse skin. In the SCC lesions, the percentage of X-Gal-positive cells was at 0.03%, which decreased in comparison with the percentage in the SCC *in situ* lesions (Figure 2C). The number of β-Gal-positive cells and total epidermal cells of the UVB-irradiated skin were as follow; dysplasia (28 of 5141), SCC *in situ* (9 of 6559), SCC (4 of 13,701).

As an additional test for BM origin, we used a mouse model in which BMDCs were GFP$^+$ using BMT from GFP transgenic mice. Although we evaluated the percentages of BMDCs in UVB-irradiated skin, the GFP$^+$/pancytokeratin$^+$ cells were found at an extremely low percentage, ~0.12% in the epidermal dysplasia lesions and 0% in the SCC *in situ* lesions (data not shown). Previous reports about the *H. felis* gastric cancer also showed a similar tendency that the percentages of malignant cells with the marker of BMDCs was much lower in GFP-labeled model mice than in β-Gal-labeled model mice.[15] Therefore we used an UVB-irradiated mouse model with labeled BMDCs with β-Gal in the following experiments.

Most BMDCs in the SCC Are Inflammatory Hematopoietic Cells

We considered that some X-Gal-positive cells in the UVB-irradiated skin were likely to be the tumor-infiltrating hematopoietic cells. To investigate the presence of these cells, triple staining for β-Gal, CD45 (hematopoietic marker), and a pancytokeratin (cytokeratin marker) was performed (Figure 3, A–C). The number of β-Gal$^+$/CD45$^+$ of all β-Gal$^+$ cells per field was counted in UVB-irradiated mouse skin. In all β-Gal$^+$ cells, 10.1% were positive for CD45 in the epidermal dysplasia lesions. Percentages of CD45$^+$ cells of all β-Gal$^+$ cells were 27.3% and 78.7% in the SCC *in situ* lesions and in the SCC lesions, respectively (Figure 3D). Some of the CD45$^+$ cells were fused with carcinoma cells. Indeed, CD45 has been found to be expressed by cancer cells.[30–32] However, we were unable to find X-Gal-positive cells that co-expressed CD45 and pancytokeratin. The result of our experiments clearly shows that some β-Gal$^+$ cells are tumor-infiltrating hematopoietic cells, whereas other β-Gal$^+$/CD45$^-$ cells might be BMDCs that differentiated into tumor keratinocytes. However, the percentage of β-Gal$^+$/CD45$^+$ cells (indicating tumor-infiltrating hematopoietic cells) is increased in the SCC lesions. This observation would indicate that the actual occurrence rate of BM-derived keratinocytes is lower than our counting of BMDCs that were detected with X-Gal staining.

Small Number of BMDCs in the SCC Exhibited Donor XY Chromosomes

To further confirm BM origin, we analyzed UVB-induced skin SCC cells from female hosts (XX chromosomes) transplanted with male donor BM (XY chromosomes) using fluorescence *in situ* hybridization technique. We counted more than 10,000 cells and detected some donor-derived keratinocytes with XY chromosome expression, indicating BM origin (less than 0.05%) (Figure 4A).

In various organs, BMDCs contribute to the tissue reconstitution by either fusion[22] or transdifferentiation.[19] To determine whether BMDC engraftment into the specific tissue cells was because of differentiation or somatic cell fusion, fluorescence *in situ* hybridization was used because the fused cells would be expected to possess XXXY chromosomes. Although we observed keratinocytes with Y chromosomes in the tumor, none of them expressed an XXXY chromosome. However, fusion hybrids notoriously lose chromosomes and the absence of tetraploid cells does not rule out fusion.[33–35] Therefore, we could not exclude the possibility of cell fusion with the present data.

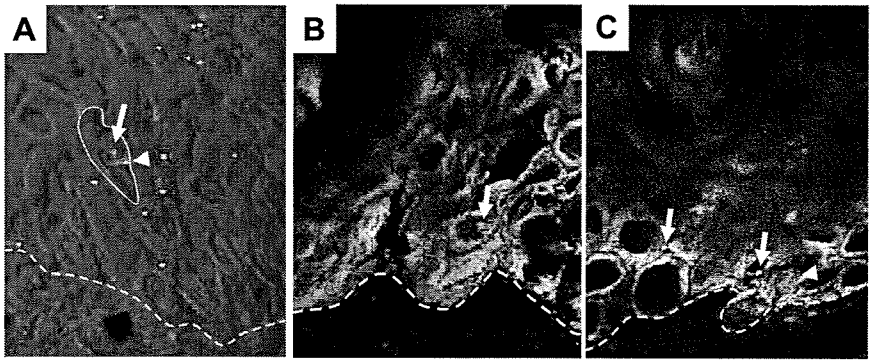

Figure 4. XY chromosome expressions and epidermal stem cell markers of the BMDCs in the UVB-irradiated skin. **A:** Fluorescence *in situ* hybridization showed cells with single X chromosome (red, **arrow**) and single Y chromosome (cyan, **arrowhead**) in the UVB-induced skin SCC. XY chromosome cells, indicating BMDCs were indicated. **B:** Triple staining of β-Gal (green), α6 integrin (red), and pancytokeratin (cyan) was performed. **Arrow** shows β-Gal$^+$ tumor keratinocytes. Although α6 integrin was positive within the edge of the tumor, we could not find any significant overexpression of α6 integrin of β-Gal$^+$/cytokeratin$^+$ cells. **C:** Triple staining of β-Gal (green), BrdU (red), pancytokeratin (cyan). **Arrows** show β-Gal$^+$ tumor keratinocytes. **Arrowhead** shows a BrdU$^+$ tumor keratinocyte. We found no β-Gal$^+$/BrdU$^+$ tumor keratinocytes.

BMDCs in the SCC Failed to Express Epidermal Stem Cell Marker

Although the CSC markers of skin SCC have yet to be defined, published studies suggest that tumor-initiating cells might be positive for the stem cell marker of the original organs.[6,8] To investigate the possibility that BMDCs in the UVB-irradiated skin could share some characteristics of CSCs of skin SCC, we assayed the location of these presumptive CSCs that are positive for epidermal stem cell markers in the UVB-induced skin SCC.

Although CD34 is an established marker of skin epithelial stem cells,[36] none of the keratinocytes (including BM-derived keratinocytes) in the UVB-induced skin SCC expressed CD34 (data not shown). Furthermore, skin epithelial stem cells express elevated levels of α6 integrin compared with differentiated keratinocytes.[37] Although some keratinocytes in the edge of SCC showed α6 integrin expression, β-Gal$^+$/pancytokeratin$^+$ cells (indicating BM-derived keratinocytes) did not show significantly upregulated α6 integrin expression compared with non-BM-derived keratinocytes (Figure 4B). In addition, tissue stem cells can be distinguished from transit-amplifying cells by their ability to incorporate and retain 5-bromo-2′-deoxyuridine (BrdU) throughout a long period of time. Therefore, tissue stem cells can be identified as label-retaining cells (LRCs).[29] To determine whether BMDCs in the UVB-irradiated mouse skin exhibit any LRC characteristics, the tumor-bearing mice were fed water containing BrdU. In the UVB-irradiated mice skin, no LRCs expressed β-Gal (Figure 4C). These results indicate that BMDCs in the UVB-induced skin SCC did not share any of these characters of the presumptive CSCs of the skin SCC.

Discussion

Based on recent investigations that suggest the possibility for BMDCs to be the origin of cancers,[15,38] we used a labeled BMDC mouse model and investigated the role of BMDCs during UVB-induced carcinogenesis. With intermittent UVB irradiation, the epidermal morphology in mouse skin changed from the normal state through dysplasia, SCC *in situ*, and finally to SCC. These histological changes are analogous to the natural phenomenon observed in UVB-induced human skin carcinogenesis. We certainly found BMDCs in UVB-irradiated mouse skin. Our data further suggests that BMDCs are recruited to the UVB-damaged skin and transdifferentiate into epidermal keratinocytes to reconstitute the skin, as we previously reported in wound repair.[20] We show the accelerated recruitment of BMDCs in the epidermal dysplasia lesions and the decreased rate of BMDCs in the SCC lesions. We propose this is attributable to the propagation of non-BM-derived malignant keratinocytes. Although BMDCs are recruited to the UVB-damaged skin and transdifferentiate into unaffected epidermal keratinocytes, BMDCs do not convert into malignant keratinocytes so that the rate of BMDCs relatively decreases as non-BM-derived tumor keratinocytes propagate to form skin SCC.

As a result, we found very few instances of BM-derived keratinocytes in the UVB-irradiated mouse skin. This observation strongly suggests that BMDCs are unlikely to be the origin of UVB-induced skin SCC. The objection will no doubt be raised that BMDCs might lose the expression of BM markers during the continuous UVB irradiation. Therefore we were careful to examine BM-derived keratinocytes in skin SCC with three different BMDC markers (β-Gal, GFP, Y chromosome analysis). Our conclusion is exactly the opposite of the *H. felis*-induced murine gastric carcinoma study.[15] It is reasonable to suppose that the difference in the results between *H. felis*-induced gastric carcinoma study and our UVB-induced skin carcinoma study is partially attributable to the process of carcinogenesis including the type of genetic damage and degree of inflammation. In *H. felis*-induced gastric carcinoma, the pathogenic factor, namely CagA, increases the proliferation of host cells or inhibits cell apoptosis, stimulating the malignant transformation of host cells.[39,40] These processes would be important for cancer progression from BMDCs. In humans, previous reports showed that solid cancers contain BM-derived cancer cells at a low level of 0 to 6% except for lung carcinoma that contains ~20% of BM-derived cancer cells.[23,24] These data further showed that BMDCs do not contribute to skin cancers.[23] Our results are consistent with these observations.

The epidermis is continuously supplied with keratinocytes from the hair follicle bulge stem cells throughout adult life.[41] Most epidermal keratinocytes that acquire

oncogenic mutations are lost during differentiation. Therefore, only long-term resident cells, such as stem cells, have the capacity to accumulate the required number of genetic hits necessary for tumor development. For this reason, it is not unreasonable to assume that these epidermal stem cells in the bulge could acquire oncogenic mutations, transdifferentiate into CSCs, and proliferate as malignant cells in the skin cancer. Although a previous report showed that BMDCs were more frequently found in the bulge area,[42] we could not find such a tendency in our experiments in UVB-induced carcinogenesis. Our previous research in the damaged skin also showed no tendency of BMDC accumulation at specific skin sites.[20] Furthermore, we failed to find any evidence of BMDC clonal expansion in the UVB-irradiated mice skin. We also showed that BMDCs express no epidermal stem cell markers and fail to behave as LRCs, one of the main characteristics of tissue stem cells. Although the existence of the CSCs in the skin cancer has yet to be properly defined, we suggest that the CSCs in the UVB-induced skin SCC, if present, do not commonly originate from BMDCs.

It is important to determine the origin of the CSCs for the elucidation of carcinogenic mechanisms or for the treatment of cancer. Because of the recent reports that showed sarcoma derived from mesenchymal stem cells,[43,44] an objection against transferring cells with the potential to have properties of stem or progenitor cells has arisen in regenerative medicine. However we can conclude from the results of our experiments that cancer cells in the UVB-induced skin SCC do not originate from BMDCs. Therefore we consider that in adopting or using BMDCs for regenerative medicine, the possibility of unexpected carcinogenesis can primarily be excluded and that BMDCs should be further tested and adapted for use in regenerative medicine, especially for skin.

We demonstrated the existence of BM-derived keratinocytes in the UVB-irradiated skin. These BM-derived keratinocytes were considered to be the result of transdifferentiation, not fusion. However, the number of BM-derived keratinocytes was extremely few, with no clonal expansion. Furthermore, BM-derived keratinocytes failed to express the epidermal stem cell markers (CD34, high α6 integrin and LRCs). Through our laboratory experiments, the possibility that BMDCs are the origin of UVB-induced skin SCC is extremely low.

References

1. Alonso L, Fuchs E: Stem cells of the skin epithelium. Proc Natl Acad Sci USA 2003, 100:11830–11835
2. Jordan CT, Guzman ML, Noble M: Cancer stem cells. N Engl J Med 2006, 355:1253–1261
3. Al-Hajj M, Clarke MF: Self-renewal and solid tumor stem cells. Oncogene 2004, 23:7274–7282
4. Lapidot T, Sirard C, Vormoor J, Murdoch B, Hoang T, Caceres-Cortes J, Minden M, Paterson B, Caligiuri MA, Dick JE: A cell initiating human acute myeloid leukaemia after transplantation into SCID mice. Nature 1994, 367:645–648
5. Cox CV, Evely RS, Oakhill A, Pamphilon DH, Goulden NJ, Blair A: Characterization of acute lymphoblastic leukemia progenitor cells. Blood 2004, 104:2919–2925
6. Singh SK, Clarke ID, Terasaki M, Bonn VE, Hawkins C, Squire J, Dirks PB: Identification of a cancer stem cell in human brain tumors. Cancer Res 2003, 63:5821–5828
7. Al-Hajj M, Wicha MS, Benito-Hernandez A, Morrison SJ, Clarke MF: From the cover: prospective identification of tumorigenic breast cancer cells. Proc Natl Acad Sci USA 2003, 100:3983–3988
8. Collins AT, Berry PA, Hyde C, Stower MJ, Maitland NJ: Prospective identification of tumorigenic prostate cancer stem cells. Cancer Res 2005, 65:10946–10951
9. Ricci-Vitiani L, Lombardi DG, Pilozzi E, Biffoni M, Todaro M, Peschle C, De Maria R: Identification and expansion of human colon-cancer-initiating cells. Nature 2007, 445:111–115
10. Li C, Heidt DG, Dalerba P, Burant CF, Zhang L, Adsay V, Wicha M, Clarke MF, Simeone DM: Identification of pancreatic cancer stem cells. Cancer Res 2007, 67:1030–1037
11. Passegué E, Wagner EF, Weissman IL: JunB deficiency leads to a myeloproliferative disorder arising from hematopoietic stem cells. Cell 2004, 119:431–443
12. Bonnet D, Dick JE: Human acute myeloid leukemia is organized as a hierarchy that originates from a primitive hematopoietic cell. Nat Med 1997, 3:730–737
13. Jamieson CHM, Ailles LE, Dylla SJ, Muijtjens M, Jones C, Zehnder JL, Gotlib J, Li K, Manz MG, Keating A, Sawyers CL, Weissman IL: Granulocyte-macrophage progenitors as candidate leukemic stem cells in blast-crisis CML. N Engl J Med 2004, 351:657–667
14. Chaligné R, James C, Tonetti C, Besancenot R, Le Couedic JP, Fava F, Mazurier F, Godin I, Maloum K, Larbret F, Lecluse Y, Vainchenker W, Giraudier S: Evidence for MPL W515L/K mutations in hematopoietic stem cells in primitive myelofibrosis. Blood 2007, 110:3735–3743
15. Houghton J, Stoicov C, Nomura S, Rogers AB, Carlson J, Li H, Cai X, Fox JG, Goldenring JR, Wang TC: Gastric cancer originating from bone marrow-derived cells. Science 2004, 306:1568–1571
16. Petersen BE, Bowen WC, Patrene KD, Mars WM, Sullivan AK, Murase N, Boggs SS, Greenberger JS, Goff JP: Bone marrow as a potential source of hepatic oval cells. Science 1999, 284:1168–1170
17. Ferrari G, Cusella G, Angelis D, Coletta M, Paolucci E, Stornaiuolo A, Cossu G, Mavilio F: Muscle regeneration by bone marrow-derived myogenic progenitors. Science 1998, 279:1528–1530
18. Brazelton TR, Rossi FMV, Keshet GI, Blau HM: From marrow to brain: expression of neuronal phenotypes in adult mice. Science 2000, 290:1775–1779
19. Harris RG, Herzog EL, Bruscia EM, Grove JE, Van Arnam JS, Krause DS: Lack of a fusion requirement for development of bone marrow-derived epithelia. Science 2004, 305:90–93
20. Inokuma D, Abe R, Fujita Y, Sasaki M, Shibaki A, Nakamura H, McMillan JR, Shimizu T, Shimizu H: CTACK/CCL27 accelerates skin regeneration via accumulation of bone marrow-derived keratinocytes. Stem Cells 2006, 24:2810–2816
21. Sasaki M, Abe R, Fujita Y, Ando S, Inokuma D, Shimizu H: Mesenchymal stem cells are recruited into wounded skin and contribute to wound repair by transdifferentiation into multiple skin cell type. J Immunol 2008, 180:2581–2587
22. Nygren JM, Jovinge S, Breitbach M, Sawen P, Roll W, Hescheler J, Taneera J, Fleischmann BK, Jacobsen SEW: Bone marrow-derived hematopoietic cells generate cardiomyocytes at a low frequency through cell fusion, but not transdifferentiation. Nat Med 2004, 10:494–501
23. Cogle CR, Theise ND, Fu D, Ucar D, Lee S, Guthrie SM, Lonergan J, Rybka W, Krause DS, Scott EW: Bone marrow contributes to epithelial cancers in mice and humans as developmental mimicry. Stem Cells 2007, 25:1881–1887
24. Avital I, Moreira AL, Klimstra DS, Leversha M, Papadopoulos EB, Brennan M, Downey RJ: Donor-derived human bone marrow cells contribute to solid organ cancers developing after bone marrow transplantation. Stem Cells 2007, 25:2903–2909
25. Gloster JHM, Neal K: Skin cancer in skin of color. J Am Acad Dermatol 2006, 55:741–760
26. Brash DE, Rudolph JA, Simon JA, Lin A, McKenna GJ, Baden HP, Halperin AJ, Ponten J: A role for sunlight in skin cancer: UV-induced p53 mutations in squamous cell carcinoma. Proc Natl Acad Sci USA 1991, 88:10124–10128
27. Katiyar SK, Korman NJ, Mukhtar H, Agarwal R: Protective effects of

silymarin against photocarcinogenesis in a mouse skin model. J Natl Cancer Inst 1997, 89:556–566
28. Allen SM, Florell SR, Hanks AN, Alexander A, Diedrich MJ, Altieri DC, Grossman D: Survivin expression in mouse skin prevents papilloma regression and promotes chemical-induced tumor progression. Cancer Res 2003, 63:567–572
29. Zhang J, Niu C, Ye L, Huang H, He X, Tong W-G, Ross J, Haug J, Johnson T, Feng JQ, Harris S, Wiedemann LM, Mishina Y, Li L: Identification of the haematopoietic stem cell niche and control of the niche size. Nature 2003, 425:836–841
30. Ngo N, Patel K, Isaacson PG, Naresh KN: Leucocyte common antigen (CD45) and CD5 positivity in an "undifferentiated" carcinoma: a potential diagnostic pitfall. J Clin Pathol 2007, 60:936–938
31. Collette M, Descamps G, Pellat-Deceunynck C, Bataille R, Amiot M: Crucial role of phosphatase CD45 in determining signaling and proliferation of human myeloma cells. Eur Cytokine Netw 2007, 18:120–126
32. Huysentruyt LC, Mukherjee P, Banerjee D, Shelton LM, Seyfried TN: Metastatic cancer cells with macrophage properties: evidence from a new murine tumor model. Int J Cancer 2008, 123:73–84
33. Pawelek JM, Chakraborty AK: Fusion of tumour cells with bone marrow-derived cells: a unifying explanation for metastasis. Nat Rev Cancer 2008, 8:377–386
34. Yilmaz Y, Lazova R, Qumsiyeh M, Cooper D, Pawelek J: Donor Y chromosome in renal carcinoma cells of a female BMT recipient: visualization of putative BMT-tumor hybrids by FISH. Bone Marrow Transplant 2005, 35:1021–1024
35. Chakraborty A, Lazova R, Davies S, Backvall H, Ponten F, Brash D, Pawelek J: Donor DNA in a renal cell carcinoma metastasis from a bone marrow transplant recipient. Bone Marrow Transplant 2004, 34:183–186
36. Tumbar T, Guasch G, Greco V, Blanpain C, Lowry WE, Rendl M, Fuchs E: Defining the epithelial stem cell niche in skin. Science 2004, 303:359–363
37. Tani H, Morris RJ, Kaur P: Enrichment for murine keratinocyte stem cells based on cell surface phenotype. Proc Natl Acad Sci USA 2000, 97:10960–10965
38. Simka M: Do nonmelanoma skin cancers develop from extra-cutaneous stem cells? Int J Cancer 2008, 122:2173–2177
39. Saadat I, Higashi H, Obuse C, Umeda M, Murata-Kamiya N, Saito Y, Lu H, Ohnishi N, Azuma T, Suzuki A, Ohno S, Hatakeyama M: Helicobacter pylori CagA targets PAR1/MARK kinase to disrupt epithelial cell polarity. Nature 2007, 447:330–333
40. Smith MG, Hold GL, Tahara E, El-Omar EM: Cellular and molecular aspects of gastric cancer. World J Gastroenterol 2006, 12: 2979–2990
41. Lavker RM, Sun T-T: Epidermal stem cells: properties, markers, and location. Proc Natl Acad Sci USA 2000, 97:13473–13475
42. Brittan M, Braun KM, Reynolds LE, Conti FJ, Reynolds AR, Poulsom R, Alison MR, Wright NA, Hodivala-Dilke KM: Bone marrow cells engraft within the epidermis and proliferate in vivo with no evidence of cell fusion. J Pathol 2005, 205:1–13
43. Tirode F, Laud-Duval K, Prieur A, Delorme B, Charbord P, Delattre O: Mesenchymal stem cell features of Ewing tumors. Cancer Cell 2007, 11:421–429
44. Aguilar S, Nye E, Chan J, Loebinger M, Spencer-Dene B, Fisk N, Stamp G, Bonnet D, Janes SM: Murine but not human mesenchymal stem cells generate osteosarcoma-like lesions in the lung. Stem Cells 2007, 25:1586–1594

Correspondence

Conradi–Hünermann–Happle syndrome with abnormal lamellar granule contents

DOI: 10.1111/j.1365-2133.2009.09110.x

SIR, Conradi–Hünermann–Happle syndrome (CHH) (X-linked dominant chondrodysplasia punctata type II, MIM 302960) is an X-linked dominant inherited disorder, characterized by linear ichthyosis, chondrodysplasia punctata, cataract and short stature.[1] The gene for this disease has been identified as EBP encoding the emopamil binding protein (EBP), located on the short arm of the X chromosome.[2,3] However, the exact pathomechanisms of how EBP defects cause the CHH disease phenotype have yet to be clarified. Ultrastructural features of CHH epidermis have thus far not been reported in patients whose EBP mutations have been identified. Here, we have ultrastructurally examined the epidermis of a patient with CHH carrying the EBP mutation p.Arg147His and have demonstrated abnormal contents of lamellar granules in the lesional granular keratinocyte layers.

A female newborn with skin scaling and shortened extremities was referred to us. The pregnancy had been uneventful except for excessive amniotic fluid, and the baby was born spontaneously at 37 weeks 4 days gestational age by normal vaginal delivery. The birth weight was 2696 g and the height at birth was 44·0 cm. No respiratory distress was observed at birth. The baby was the second child of nonconsanguineous, healthy parents. There was no other affected member in the family, including the proband's healthy elder brother. Frontal bossing, flat nasal bridge and shortened neck were noted at birth (Fig. 1). The right upper and lower extremities of the patient were shortened. Whole body X-ray examination revealed punctate calcification in the epiphyseal regions of the majority of long bones (Fig. 1), including shoulder joints, elbow joints, wrist joints, hip joints, knee joints and ankle joints, and the calcification was most severe on the right side of her body. Her height was below the third percentile at birth and during all the postnatal period. Her weight was also below the third percentile from 2 months of age, although it was between the 10th and the 25th percentile at birth. She had bilateral anterior polar cataracts, which were more severe on the right side. During the neonatal period, linear and whorled hyperkeratosis was seen on erythrodermic skin and the thick scales were more severe on the right side of her

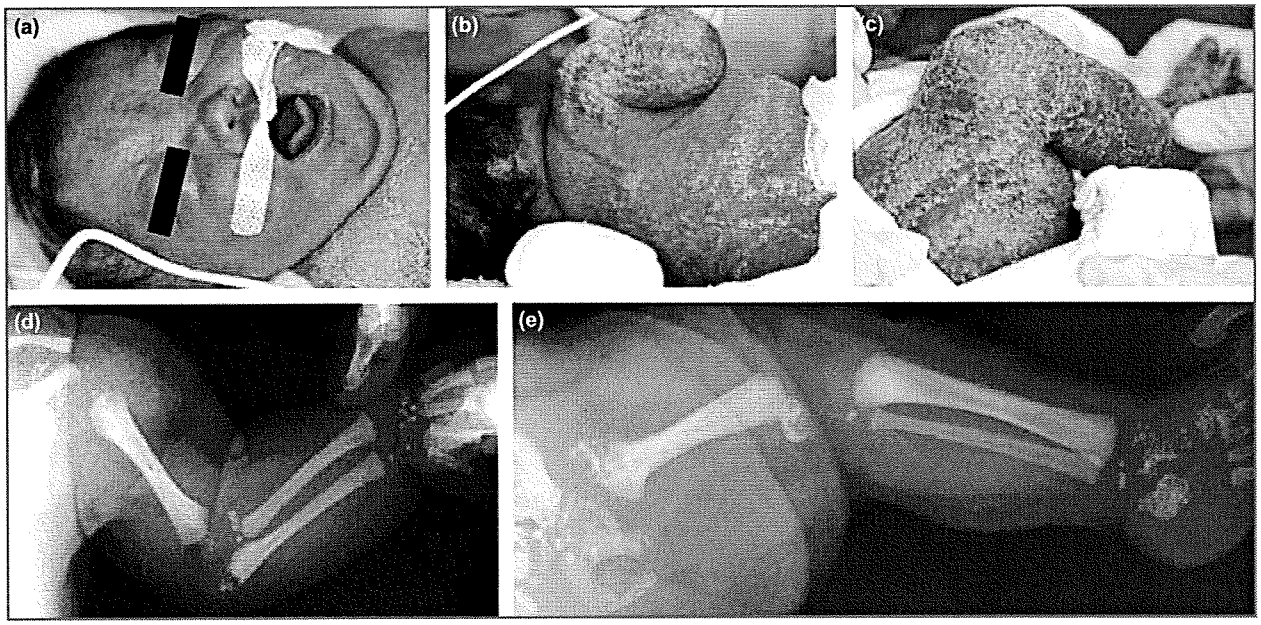

Fig 1. Clinical and X-ray appearance of the patient. (a) Frontal bossing and flat nasal bridge were seen on the face. (b) Circumscribed alopecia was noted on the scalp. (b, c) Linear and whorled hyperkeratosis was seen on a background of erythrodermic skin on the back (b) and over the thigh (c). (d, e) X-ray showed punctate calcification in the epiphyseal growth plate of the bones of the right arm (d) and in the right leg and hip (e).

© 2009 The Authors
Journal Compilation © 2009 British Association of Dermatologists